LIBRARY
CALIFORNIA AIR RESOURCES BOARD
P.O. BOX 2815
SACRAMENTO, CA 95812

APPLICATION OF ATMOSPHERIC TRACER TECHNIQUES TO DETERMINE THE TRANSPORT AND DISPERSION ASSOCIATED WITH THE LAND-BREEZE MOVEMENT OF AIR OVER THE LOS ANGELES COASTAL ZONE

VOLUME 2

EXTENDED SUMMARY AND ANALYSES OF SPECIAL TOPICS

by

Fredrick H. Shair

Division of Chemistry and Chemical Engineering

California Institute of Technology

Pasadena, California 91125

Prepared for the California Air Resources Board

December 2, 1982

A6-202-30
OR
A6-202-32

Table of Contents

Introduction

Seven large scale atmospheric tracer studies, using SF6, were conducted in order to probe the transport and dispersion associated with the Los Angeles land breeze-sea breeze circulation system. The details of the release information, as well as the tracer data are presented in Volume 3.

Tests 1 and 2 involved releasing SF6 for a 5-hour period during each of two nights from stack #4 of the power plant operated by the Southern California Edison Company. Even though a portion of the plume was apparently injected above the base of the nighttime inversion, essentially all of the tracer was observed to return across a control surface (from sea level to the base of the inversion) along the coast throughout the sea breeze regime during the following day. The residence time distribution functions of tracer material over the sea were almost identical in both experiments. The average residence time for tracer material over the ocean was 10 hours in both cases; however, some of the tracer spent as much as 16 hours out over the sea. The horizontal dispersion of tracer was also greater than had been expected, with between 75 and 100 km of coastline impacted by the return of SF6 from a single elevated point source. Data from both shipborne and coastal monitoring stations indicate that the

path followed by the tracer over the ocean could not have been tracked accurately using trajectories constructed from conventionally available meteorological data. The results of tests 1 and 2, including discussions of the physics of the fumagation processes, are contained within chapter 1 which has been reviewed and accepted for publication in the Atmospheric Environment Journal.

Chapter 2 contains the mathematical formulation of a model of the fumagation process. The model considers the following to occur: During the night, cool stable air is advected out over the ocean. When this air encounters the warmer ocean surface, convective mixing begins to erode the stable layer. Once the internal boundary layer has grown to the height of the plume, the tracer material, entrained at the top of the of the mixed layer, is rapidly fumigated to the surface.

The calculated characteristic time for downmixing, (based upon the gradient Richardson Number, the Monin-Obukuhov length and turbulence intensities), is of the order of 20 minutes for the conditions associated with the tests 1 and 2. This result is in good agreement with that inferred from the tracer concentration records obtained onboard the Acania Research Vessel. This chapter has been reviewed and has been accepted for publication in the Journal of Applied Meteorology.

Chapter 3 contains an analysis of the sulfate formation associated with the land breeze-sea breeze circulation system probed with the tracer in tests 1 and 2. The tracer results in tests 1 and 2 suggest that there is a significant increase in the time available for sulfate formation in the marine environment due to the fact that the air makes multiple passes over heavy emissions along the coast. Sulfur oxides recirculated by the previous night's land breeze were found to be the largest single contributor to 24 hour average sulfate concentrations during tests 1 and 2. In contrast, 24 hour average SO2 concentrations were dominated by fresh emissions from nearby sources. These calculations indicate that the overall rate of SO2 oxidation to form sulfates in the Los Angeles atmosphers is about 6% per hour during the summer. Thus,if large reductions in sulfate concentrations are sought, it will be necessary to reduce sulfur dioxide emissions even during the night when an off-shore breeze is present.

A brief discussion concerning the influence of the Los Angeles sea breeze-land breeze is presented in Chapter 4 which was reprinted from the proceedings of the Second Joint Conference on Applications of Air Pollution Meteorology and Second Conference on Industrial Meteorology, held during 24-28 of March 1980.

Chapter 5 contains the methodology for calculating mass balances and the associated uncertainties inherent in field data. For the cases studied (i.e. tests 1 and 2) the nominal values for the mass of tracer returned across the control surface were in good agreement with those released into the land breeze; that is, essentially all of the tracer was accounted for in both tests 1 and 2. In these cases the total uncertainties in the nominal values (about 25%) were substantially less than the uncertainty in any individual measurement of concentration, wind speed or mixing height (30%-40%). This result is simply a reflection of the effect of statistical cancellation of errors distributed randomly about the actual value of the measured variables.

Chapter 6 contains the sulfate data which was used in the analysis associated with chapter 4; these data were collected by the aerosol studies section of the Research Division of the ARB.

Further analyses of the data associated with tests 3-7 and associated manuscripts are anticipated; however, this report is thought to clearly meet the objective of the ARB grant and, as such, represents the final report. Other manuscripts will be sent when they are finished, as a matter of courtesy.

Chapter 1

TRANSPORT AND DISPERSION OF AIRBORNE POLLUTANTS ASSOCIATED WITH THE LAND BREEZE-SEA BREEZE SYSTEM

by

F. H. Shair, E. J. Sasaki and D. E. Carland
Chemical Engineering

G. R. Cass and W. R. Goodin*
Environmental Quality Laboratory

California Institute of Technology
Pasadena, California 91125

J. G. Edinger
Department of Atmospheric Sciences
UCLA
Los Angeles, California 90024

and

G. E. Schacher
Department of Physics and Chemistry
Naval Postgraduate School
Monterey, California 93940

October 1981

*Present affiliation: Dames & Moore, 1100 Glendon Avenue
Los Angeles, California 90024

In press, Atmospheric Environment

ABSTRACT

Two atmospheric tracer experiments were conducted in July 1977. SF_6 was released for a 5-hour period during each of two nights from a coastal power plant stack located at the El Segundo Generating Station in the Los Angeles Basin. The purpose of this study was to investigate the transport and dispersion of plumes released into the land breeze portion of a land breeze/sea breeze circulation system. Even though a portion of the plume was apparently injected above the base of the nighttime inversion, essentially all of the tracer was observed to return across a control surface (from sea level to the base of the inversion) along the coast throughout the sea breeze regime during the following day. The residence time distribution functions of tracer material over the sea were almost identical in both experiments. The average residence time for tracer material over the ocean was 10 hours in both cases; however, some of the tracer spent as much as 16 hours out over the sea. The horizontal dispersion of tracer was also greater than expected, with between 75 and 100 km of coastline impacted by the return of SF_6 from a single elevated source. Data from both shipborne and coastal monitoring stations indicated that the path followed by the tracer over the ocean could not have been tracked accurately using trajectories constructed from conventionally available meteorological data.

1. Introduction

Coastal emission sources present special difficulties for air quality control programs because of the complexities associated with coastal meteorological processes. Differential heating of land and sea surfaces often generates an inland flow of air during the daylight hours. However at night, the land cools faster than the sea, and the wind may reverse direction. The fate of pollutants emitted into the nighttime offshore breeze is difficult to evaluate using conventional air quality models because of the lack of meteorological data needed to describe the flow reversal and mixing processes over the water.

The objective of the present study was to explore the transport and dispersion of elevated plumes released into the land breeze portion of a land breeze/sea breeze circulation system. An inert gaseous tracer, SF_6, was used to determine the extent to which pollutants sent seaward at night from elevated coastal Los Angeles emission sources by a land breeze could return to the Los Angeles region at ground level during the next day's sea breeze. Multiple passes of the same air mass over coastal emission sources could lead to pollutant accumulation in the air basin of interest. In order to gauge the potential magnitude of this accumulation problem, the fraction of the emissions into the land breeze that returned the next day was determined, along with the degree of dilution observed and the retention time available for chemical reaction of pollutants while they resided in the marine environment.

2. Previous Studies of Land-Sea Breeze Transport Phenomena

Land-sea breeze circulation systems-- their extent, duration, frequency and intensity have been studied for many years (see for example Eatontown Signal Laboratory Group, 1945; Defant, 1951; Kraus, 1972; Scorer, 1978). It has been shown that sea breeze/land breeze systems influence air pollutant transport over the Great Lakes and East Coast regions of the United States (Lyons and Olsson, 1973; Lyons, 1975; Raynor et al. 1975; Lyons and Keen, 1976; SethuRaman and Raynor, 1980). But perhaps the most widely studied coastal breeze system is that associated with the Los Angeles region. Beginning in the late 1940's it was realized that the sea breeze portion of this coastal meteorological phenomenon dominates air pollution transport across the Los Angeles Basin (Beer and Leopold, 1947; Kauper, 1960; Taylor, 1962; DeMarrais, Holzworth and Hosler, 1965). In succeeding years, air pollution aspects of the Los Angeles land-sea breeze system have been explored by trajectory calculations, tetroon flights, fluorescent particle releases and SF_6 tracer studies.

Early studies of air parcel transport in the Los Angeles Basin were based on trajectories constructed from surface wind data (Edinger, 1948; Neiburger and Edinger, 1954; Neiburger, Renzetti and Tice, 1956; Taylor, 1962). Emphasis was placed on inland sea breeze transport of photochemically-reacting pollutants. Forward and backward trajectories were calculated between major source areas and inland receptor points such as downtown Los Angeles. In the absence of routine meteorological measurements over the ocean, only a few studies paid attention to the

fate of materials transported seaward by the land breeze. Kauper (1960) analyzed meteorological and air quality data from a day during which the measured oxidant concentration exceeded 0.5 ppm in the afternoon at the coast near El Segundo. His conclusion was that transport of oxidant precursors offshore by the land breeze and subsequent reaction and onshore transport of oxidant by the following sea breeze caused the high concentration of pollutants observed at the coast. Kauper and Niemann (1975, 1977) conducted two studies to characterize interbasin pollutant transport. Their analyses utilized extensive pibal, surface, aircraft, and ship data to calculate the path of specific "parcels" of air as they moved from the Los Angeles Basin over water to downwind receptors. They concluded that high ozone levels measured at Oxnard during June and July, 1975, and at San Diego during October, 1976, were the result of ozone transport aloft from the Los Angeles Basin.

In order to study transport into zones of sparse meteorological data, tracer techniques can be employed. Holzworth, Kauper and Smith (1963) released three tetroons from downtown Los Angeles on a summer day and tracked their movement visually along generally inland trajectories. Pack and Angell (1963) released 88 tetroons from nine Los Angeles area coastal sites into both land and sea breeze flows and tracked their motion using radar mounted on Catalina Island. Of special interest were 4 releases made from Long Beach during two successive nights. One of the tetroons moved parallel to the coastline before being transported inland at about 4 a.m.; a second one spent the nighttime hours over water before recrossing the coastline at dawn,

while two of the four tetroons moved seaward and spent considerable time over water before recrossing the coastline the next day with the afternoon sea breeze. Angell et al. (1972) monitored the three-dimensional motion of tetroons over the Los Angeles Basin. Most of those releases were into the sea breeze although the balloons were tracked at all hours of the day and night. They concluded that during the day, trajectories computed from surface wind data provide a reasonably good estimate of the motion in the lowest few hundred meters of the atmosphere. However, at night the situation is much more complex due to the presence of substantial wind shear in the vertical direction. As a result, quantitative evaluation of pollutant transport and dispersion processes that occur at night over the ocean will have to proceed by means other than surface wind trajectory calculations.

Information on pollutant dispersion can be derived from tracer experiments that employ fluorescent particles or SF_6. Fluorescent particle studies attempted in the Los Angeles area have met with mixed results. The fraction of the fluorescent tracer material released which can be accounted for at monitoring sites is often quite low, as experienced by Kauper, Holmes and Street (1955). Neiburger (1955) designed an experiment in which fluorescent particles were released into the Los Angeles nighttime land breeze, but the fate of the particles released could not be determined. Vaughan and Stankunas (1974) released fluorescent particles during the morning of seven days between the summer of 1972 and the fall of 1973. They obtained no information concerning the fate of emissions transported seaward at night.

Sulfur hexafluoride gas (SF_6) is a much better tracer than fluorescent particles when attempting to characterize the transport and dispersion of gaseous pollutants. SF_6 is detectible at concentrations less than one part in 10^{12} parts air. Ground level dry deposition, which adversely affects recovery of fluorescent particles, is eliminated because SF_6 is an inert gas. Drivas and Shair (1974, 1975) and Lamb et al. (1977) have employed SF_6 to investigate transport and dispersion of gaseous pollutants during daytime sea breeze conditions in the Los Angeles area. The nighttime seaward transport and dispersion characteristics within land-sea breeze systems remain to be determined.

3. Experimental Design and Procedures

On two occasions during July 1977, SF_6 tracer was released late at night into the stack of Unit 4 at the Southern California Edison Company's El Segundo Generating Station. Pilot balloon observations made at Hermosa Beach prior to each release indicated that an offshore land breeze set up aloft above 300 meters around midnight on these occasions and propagated downward with time. Tracer releases were initiated after the offshore flow was confirmed to exist at and above about 200 m in elevation. During Test 1, SF_6 was released at a rate of 5.0 g s^{-1} from 0005 hours to 0500 hours PDT on July 22, 1977. Test 2 occurred at an SF_6 release rate of 13.6 g s^{-1} from 2303 hours PDT July 23, 1977 until 0400 hours PDT July 24, 1977.

Prior to each release, SF_6 sampling was initiated aboard the U.S. Navy Research Vessel Acania as it cruised in a zig-zag pattern across the Santa Monica Bay downwind of the tracer release point. Air samples of 10-second duration were taken at one to five minute intervals using 30 cm^3 plastic syringes. Portable electron capture gas chromatographs placed onboard the ship permitted rapid feedback of tracer concentration information during each test. A description of electron capture detection of SF_6 is provided elsewhere (Drivas, 1974; Lamb et al. 1977). Calibration results show that SF_6 concentrations down to 10^{-12} parts SF_6 per part air are readily detected. For comparison, if the total amount of tracer released during each test were uniformly distributed throughout an air volume of 40 km by 40 km by 300 m (i.e. the air volume over the entire Santa Monica Bay from the sea surface to above the effective stack height of the power plant), then the average tracer concentrations would have been about 29 and 78 ppt for Tests 1 and 2 respectively. Ability to detect the power plant plume if encountered at the sea surface thus was reasonably assured.

Tracer releases were halted when the land breeze subsided. In anticipation of a reversal in wind direction associated with the following sea breeze, SF_6 sampling then was initiated at a network of 29 fixed coastal monitoring sites located from Ventura to Corona del Mar (see Fig. 1). Hourly average samples were collected consecutively from 0500 to 1700 hours PDT at these coastal fixed sites during both

tests. SF_6 concentrations also were monitored hourly from July 19 through July 29 at Santa Catalina Island.

Automobile sampling traverses were conducted periodically along coastal highways between 1000-1427 hours PDT July 22 and between 0235-1540 hours PDT July 24. Grab samples were collected at 0.8 to 3.2 km intervals along coastal U.S. Highway 1 between Redondo Beach and Malibu, and along Interstate Highway 405 between the San Fernando Valley and either the Long Beach harbor area or northern Orange County. The purpose of the coastal fixed samplers and highway traverses was to assess the time and place at which pollutants sent seaward at night were returned back across the coastline.

Meteorological data were collected both at sea and on land during each test in order to assist explanation of the tracer concentrations observed. The depth of the mixed layer above the sea surface over Santa Monica Bay was established by continuous acoustic sounder recordings made aboard the R.V. Acania. Vertical temperature profiles up to 1000 m altitude were obtained by radiosondes released from the ship at 0200 hours, 0600 hours and 0900 hours PDT on both July 22 and July 24. In addition, the Acania was equipped with two masts instrumented to measure wind speed, temperature, dew point/humidity, temperature fluctuations and wind speed fluctuations at elevations of 4.2 m, 7.0 m, 14.7 m and 20.5 m above the sea surface. Sea surface temperature was monitored from a boom extending 3.1 m in front of the ship's bow. Meteorological data taken aboard the Acania are presented

by Schacher et al. (1978, 1980). The ship's instrumentation is described in detail by Houlihan et al. (1978).

Data on winds aloft were gathered from a limited number of pibal releases conducted at Hermosa Beach near the point of tracer injection. Pilot balloons were launched at 5 times from 2100 hours PDT on July 21 through 0400 hours PDT on July 22, and at 9 times from 2100 hours PDT on July 23 through 0540 hours PDT on July 24. Wind speed and direction were recorded at 100 m intervals above sea level. Low strata inhibited the use of pibals at altitudes greater than 400 to 600 m on several occasions. Hourly observations of surface wind speed and direction can be obtained in the Los Angeles area at more than 50 land-based meteorological stations operated by the National Weather Service, local air pollution control districts, the California Air Resources Board and the U.S. Navy.

4. Tracer Test Results

Test 1 July 22, 1977

Pibal observations taken at Hermosa Beach at 2100 hours PDT on July 21 showed an onshore flow at the surface with an offshore flow aloft above 500 m elevation. By 2200 hours on that day, the land breeze had propagated downward to about 300 m elevation. Shortly before midnight, the land breeze was observed at the ocean's surface aboard the Acania as it cruised less than 10 km seaward from El Segundo. Starting at 0005 hours PDT on July 22, the SF_6 tracer was released into the offshore flow from the El Segundo power plant stack.

Radiosonde measurements taken at the ship at 0200 hours PDT showed that a strong temperature inversion based at between 200 and 240 m elevation existed over the Acania at that time. The acoustic sounder indicated the depth of the mixed layer to be about 200 m at 0000 PDT July 22. From that time until 0630 PDT the depth of the mixed layer above the ship remained at or below about 220 m (with the exception of a single value of 250 m recorded at 0220 hours PDT). At 0630 PDT, the top of the mixed layer rose above 220 m, and remained between 220 m and 280 m until noon (again with the exception of one measurement at about 200 m depth).

The trajectory of the SF_6 plume over the Santa Monica Bay was estimated from available meteorological data. Streaklines corresponding to plume centerlines were constructed from sparse upper level pibal data. Using Briggs' (1971) plume rise formula, the effective stack height of the power plant was estimated to be approximately 250 m. Plume rise calculations by the method of Schatzmann (1979) yield similar results (McRae et al, 1981). Thus during the SF_6 release, it appears that the plume would have risen at least to the base of the temperature inversion and possibly into the stable air mass within the inversion. Because of the uncertainties associated with plume rise calculations, possible plume trajectories in the horizontal plane were computed using pibal observations from two heights, 108 m and 315 m. Pibal measurements taken on the hour were assumed to apply to the following full hour. Surface wind data were used to compute horizontal transport for comparative purposes.

SF_6 tracer concentrations measured aboard the Acania and estimated plume locations are compared in Figure 2. On three occasions prior to 0530 PDT, the ship passed beneath the computed location of the plume: at about 0100 hours, between 0300 and 0330 hours, and again between 0430 and 0500 hours PDT. The mixing depth on all three occasions was below 200 m and no significant concentrations of SF_6 were detected, except that as the ship passed beneath the plume at 0325 and at 0437 PDT, very small amounts of SF_6 were detected (14 ppt and 11 ppt, respectively). At 0220 hours when the mixing depth above the ship briefly exceeded 220 m, the ship was located far to the south of the likely location of the plume.

Between 0530 and 0545 PDT, the first significant peak in SF_6 concentration (80 ppt) was recorded at the ship. At this time the top of the mixed layer was rising toward the 200 m level. The ship was well south of the plume centerline computed from 100 m wind data. Trajectories computed from 300 m winds would place the plume in the vicinity of the ship at that time.

At 0615 PDT the ship moved northward to recross the path of the plume. Between 0620 and 0640 PDT the depth of the mixed layer increased to 240 m. Shortly thereafter high concentrations of SF_6 were measured at sea level as the ship passed beneath the computed location of the plume. From 0830 until 1130 PDT the ship saw no less than 18 ppt of SF_6 at the sea surface as it cruised across the central portion of the Santa Monica Bay.

Between 0700 and 0800 hours PDT, net onshore sea breeze flow was established along the coastline from Ventura to northern Orange County. SF_6 concentrations greater than 10 ppt were first observed in air recrossing the coast between 0900 and 1000 PDT. For the next 8 hours, SF_6 continued to cross the coastline from north of Pt. Mugu to as far south as Long Beach, a distance of roughly 100 km, as shown in Figure 3.

SF_6 Mass Balance Calculations

In order to determine the residence time distribution of the stack gases within the marine environment, a mass balance was constructed for the flux of SF_6 tracer returning landward during the day following each tracer release. A control surface, generally paralleling the coastline, was constructed from seven straight line segments attached end to end such that each segment traversed a zone of common topographic conditions, as listed in Table 1. Surface wind stations lying along each stretch of coastline were reviewed. A station or pair of stations was chosen to represent air mass motion along each section of the control surface, as listed in Table 1. Whenever possible, the average of the wind speed and direction measured at two wind stations located as far apart as possible along each stretch of coastline was employed to estimate average air velocity along that entire coastal segment. This was done in order to reduce the effect of errors in a single wind station's record that could affect the large air fluxes calculated across coastal flatlands.

Wind vectors apparent at each hour along each segment of the control surface were resolved into their components normal to the coast. The distance that the wind penetrated across each stretch of coastline during each hour was defined in this manner. Using the length of each control surface segment as a crosswind dimension, and the mixing depth data from the Acania as a vertical dimension, the volume of air crossing the coast within the surface mixed layer was determined at each hour.

The control surface parallel to the coast was subdivided into short intervals approximately centered on each SF_6 monitoring site. This subdivision was accomplished by bisecting the distance between each adjacent pair of SF_6 sampling stations and then drawing a line perpendicular to the control surface from the midpoint between each pair of monitoring sites. In that manner, the volume of air crossing the coast during each hour was apportioned between SF_6 monitoring sites.

The SF_6 concentration averaged over each hour at each sampling station was assumed to represent the average concentration of SF_6 in the air flow assigned to the coastline interval surrounding it. SF_6 concentrations shown in Figure 3 were then converted to SF_6 mass fluxes within the surface mixed layer of the atmosphere crossing each coastal interval at each hour. By summing these SF_6 fluxes, a mass balance for SF_6 released and recovered was constructed, and the residence time distribution of the tracer and associated emissions over the ocean was determined.

The results of the SF_6 mass balance from Test 1 are shown in Figure 4a. These calculations indicate that essentially all of the SF_6 released into the land breeze at night was observed to recross the coastline of the air basin within the surface mixed layer during the following day's sea breeze regime. Sixty-nine percent of the tracer material recrossed the Los Angeles County coastline along the Santa Monica Bay (near the release point), while thirty-one percent of the SF_6 returned across the Ventura County coastline near Oxnard to the north. Transport of such a large fraction of the tracer material northward into Ventura County would not have been predicted from trajectories drawn from available surface wind data.

Test 2 July 24, 1977

At 2200 hours PDT July 23, pilot balloons released from Hermosa Beach showed an onshore flow at 108 m elevation with offshore flow aloft at and above 216 m elevation. One half hour later, pibal observations indicated that the land breeze existed at 108 m elevation and above. At 2303 hours PDT the second release of tracer was begun from the power plant stack.

The first acoustic sounder measurements made following the start of this experiment place the base of the sub-tropical inversion at about 500 m above the Acania. A strong temperature inversion at that elevation persisted throughout the night as shown by both the acoustic sounder and the radiosondes taken at 0200 plus 0600 PDT. Between 1000 and 1100 hours PDT, the inversion base dropped from around 500 m to about 300 m elevation, then returned to 500 m briefly before

stabilizing at a height between 260-350 m during the rest of the experiment.

Possible plume trajectories in the horizontal plane were computed using pibal observations at 108 m and 315 m elevations plus surface wind data. In Figure 5, SF_6 concentration measurements obtained aboard the Acania are co-ordinated with the ship's position and possible plume centerline locations. SF_6 was first observed at the sea surface aboard the Acania at 0144 hours, reaching a short term peak of 59 ppt at 0152 hours while the ship was very close to the coast at Santa Monica. Low levels of tracer were measured at the ship almost continuously thereafter. SF_6 was first observed at the surface at the coast from Santa Monica to Carbon Canyon Road (near Malibu) between 0250 and 0330 PDT during two automobile traverses along Highway 1. Concentrations up to 64 ppt SF_6 were found ashore at a point closely corresponding to the end point of the plume trajectory computed from 100 m winds shown in Figure 5.

At 0400 hours, the plume trajectories computed from Hermosa Beach pibal data and surface winds would suggest that the plume was confined to an area over Santa Monica Bay within 15 km of the coastline to the north and west of the release point. SF_6 measurements obtained aboard the Acania, however, show a quite different picture. The Acania first encountered high SF_6 concentrations (up to 461 ppt) shortly after 0400 hours PDT at a location well west of the plume trajectory computed from 300 m winds. After apparently crossing through the plume at about 0415 PDT, SF_6 concentrations dropped to a low of 34 ppt. The ship then

executed a series of turns and eventually headed in a southeast direction parallel to the El Segundo coastline at a distance of about 20 km offshore. SF_6 concentrations at the ship were observed to increase continuously from 0600 hours to 0800 hours to levels above 250 ppt, although the ship was west or south of the computed position of the plume at most times. Southward motion of a portion of the plume over the ocean also is confirmed by the SF_6 monitoring station at Santa Catalina Island which recorded SF_6 concentrations up to 36 ppt briefly during the period 1200-1500 hours PDT.

Onshore flow was already apparent at the coast from Malibu southward when sampling commenced at 0500 hours at the coastal fixed monitoring stations. As in Test 1, the tracer material was observed to be transported over long distances within the marine environment before recrossing the coast the next day. In this case, the predominant direction of flow was more northerly (toward the south) than encountered during Test 1. Tracer material was measured recrossing both the Santa Monica Bay and Long Beach portions of the Los Angeles County coast, as well as along the Los Alamitos to Newport Beach stretch of the coast of Orange County to the south of Los Angeles (see Figure 6).

A mass balance for SF_6 released versus that returned inland by the sea breeze was constructed by methods previously described. The acoustic sounder showed a weak intermittent return during Test 2 at an elevation below the location of the sub-tropical inversion base. Mass balance calculations using that return height as a mixing depth would

indicate a 49% recovery of the tracer released. Careful reexamination of the acoustic sounder records indicates that the sub-tropical inversion base was the true limit to vertical dispersion in this case. Using the base of the sub-tropical inversion as as estimate of the mixing depth during Test 2, 244 kg of SF_6 (essentially all of the SF_6 released) would have recrossed the coastal monitoring network (as shown in Figure 4b).

It is clear that selection of wind stations and mixing depths influences mass balance results. A sensitivity analysis of mass balance results was conducted independently by Sackinger et al. (1981). Their calculations also indicate that the great majority of the tracer material sent seaward at night during both Tests 1 and 2 returned inland the next day with the sea breeze.

5. Summary and Discussion

Results from both Tests 1 and 2 show that a major portion of the tracer material released into a land breeze at night from an elevated coastal emission source was advected back over the coast during the following day's sea breeze. Multiple passes of the same air mass over coastal point sources thus leads to pollutant accumulation within the Los Angeles basin.

The retention time for pollutants within the marine environment during these tests can be estimated from Figures 4a and 4b, and is shown in Figure 7. When normalized on the basis of the total amount of SF_6 returned to land, the residence time distributions for SF_6 over the

ocean during Tests 1 and 2 are remarkably similar. The median age of the material returned to land was about 10 hours in both tests. On a first in/last out basis, some of the emissions could have been retained over the ocean for up to 16 hours. Even relatively slow chemical reactions involving pollutants trapped in such a land/sea breeze circulation system would have considerable time to proceed toward completion before emissions returned to encounter receptor populations.

Dispersion of tracer material during these tests was much greater than expected. The tracer dosage accumulated along the coastal monitoring sites is given in Figure 8, and shows that SF_6 released into the land breeze from a single source crossed between 75 and 125 km of coastline during the following day's sea breeze. During both tests, at least some tracer material was found in the vicinity of trajectories drawn from surface or upper level wind data. But in both cases, the northward or southward edge of the returning tracer cloud was much farther from the release point than would be indicated by trajectories drawn from pibal releases made near the source. During Test 1, two pronounced peaks in SF_6 mass were observed to be crossing the coast simultaneously (see Figure 3), one near the SF_6 release point and another far to the northwest near the Ventura/Los Angeles County line. This plume apparently was dispersed by wind shear over the Santa Monica Bay.

In the case of Test 1, a description of transport and dispersion processes can be provided which is compatible with shipboard observations of SF_6 concentrations, mixing heights, inversion height,

and data on winds aloft. The essential features are:

(a) The heated plume from the stack rises to the base of the inversion where it arrives still a little warmer than the ambient air but not as warm as the air a short distance above. The plume levels out at this height and partially penetrates the base of the inversion. The coolest plume material is below the inversion base and the warmest just above. Stronger winds aloft carry the upper parts of the plume farther out to sea than the lower portion which moves more nearly with the surface wind field.

(b) A mixed layer begins forming at the sea surface as air, previously cooled by contact with the nocturnally cooled land surface, crosses the coastline on the land-breeze and encounters the warmer ocean surface. The convectively mixed layer which develops grows in thickness as the heating from below continues, and in time the top of this mixed layer approaches the base of the inversion.

(c) Upon reaching the lower edge of the plume, the convective mixing motions fumigate SF_6 down to the sea surface. This fumigation process accounts for the observation that the SF_6 suddenly appeared at the sea surface after 0500 PDT but was not observed during three prior ship passages beneath the plume earlier in the experiment. Fumigation continues as long as plume material remains near the base of the inversion, in time distributing it almost uniformly from sea surface to inversion base. A detailed quantitative treatment of the convective downmixing processes

which act on the plume during this experiment is provided by McRae et al. (1981), and shows that the time scales for convective mixing during this experiment are consistent with the above fumigation hypothesis.

(d) The plume material begins moving back toward land when the seaward limit of the land breeze begins to move toward land as the morning sea breeze develops. This zone of convergence between the land- and sea-breeze produces a swelling of the sub-inversion layer and can propagate through the atmosphere at speeds exceeding the sea breeze. The ship passed through this zone at 0735 PDT at which time the maximum mixing height, 280 m, was observed at the ship.

Results obtained during Test 2 would not have been explained by an air quality model using commonly available meteorological measurements. In particular, transport of material southward to Santa Catalina Island, Newport Beach and Corona Del Mar would not have been predicted from pibals launched near the SF_6 release point or from trajectories drawn from surface wind data. Uncertainties in the mixing depth estimates would have further complicated pollutant concentration calculations. Under these circumstances, a tracer like SF_6 is essential to an assessment of pollutant transport and dispersion.

Acknowledgement

The advice and assistance furnished throughout this program by Charles Bennett is gratefully acknowledged. The cooperation of the Southern California Edison Company is also appreciated. This work was supported by the California Air Resources Board under agreement A6-202-30.

REFERENCES

Angell J.K., Pack D.H., Machta L., Dickson C.R. and Hoecker W.H.(1972) Three-dimensional air trajectories determined from tetroon flights in the planetary boundary layer of the Los Angeles basin. J. Appl. Met. 11, 451-471.

Beer C.G.P. and Leopold L.B. (1947) Meteorological factors influencing air pollution in the Los Angeles area. Trans. Amer. Geophysical Union 28, 173-192.

Briggs G.A. (1971) Plume rise: a recent critical review, Nuclear Safety 12, 15-24.

Defant F. (1951) Local winds, in Compendium of Meteorology, Amer. Met. Soc., Boston, Mass., 655-662.

DeMarrais G.A., Holzworth G.C. and Hosler C.R. (1965) Meteorological summaries pertinent to atmospheric transport and dispersion over southern California, Report No. 54, U.S. Weather Bureau, Washington, D.C., 90 pp.

Drivas P.J. (1974) Investigation of atmospheric dispersion problems by means of a tracer technique, Ph.D. Thesis, California Institute of Technology, Pasadena, California, 91125.

Drivas P.J. and Shair F.H. (1975) The chemistry, dispersion and transport of air pollutants emitted from fossil fuel power plants in California-Transport of plumes associated with the complex coastal meteorology, Division of Chemistry and Chemical Engineering, California Institute of Technology, performed under California Air Resources Board Contract No. ARB-915.

Drivas P.G. and Shair F.H. (1974) A tracer study of pollutant transport and dispersion in the Los Angeles area. Atmospheric Environment 8, 1155-1163.

Eatontown Signal Laboratory Group (1945) Local Winds -- mountain and valley winds, land and sea breezes, Report No. 982, U.S. Army Signal Corps, Dugway Proving Grounds, Tooele, Utah, 50 pp.

Edinger J.G. (1948) A study of air flow in the Los Angeles basin, Meteorology Department, UCLA, June, 106 pp.

Holzworth G.C., Kauper E.K. and Smith T.B. (1963) Some observed low-level air trajectories over Los Angeles, California. Mon. Wea. Rev. 91, 387-392.

Houlihan T.M., Davidson K.L. Fairall C.W. and Schacher G.E. (1978) Experimental aspects of a shipboard system used in investigation of overwater turbulence and profile relationships, Naval Post Graduate School Report No. NPS 61-78-001, Monterey, California.

Kauper E.K., Holmes R.G. and Street A.B. (1955) The verification of surface trajectories in the Los Angeles basin by means of upper air observations and tracer techniques, Tech. Paper No. 14, Air Pollution Control District, Los Angeles, California, 19 pp.

Kauper E.K. and Niemann B.L. (1975) Los Angeles to Ventura over water ozone transport study, Metro Monitoring Services, Covina, California, 51 pp.

Kauper E.K. (1960) The zone of discontinuity between the land and sea breeze and its importance to southern California air pollution studies, Bull. Amer. Met. Soc. 41 410-422.

Kauper E.K. and Niemann B.L. (1977) Los Angeles to San Diego three dimensional ozone transport study, Metro Monitoring Services, Covina, California, 43 pp.

Kraus, E.B. (1972), Atmosphere-Ocean Interaction, Clarendon Press, Oxford, 275 pp.

Lamb B.K., Lorenzen A. and Shair F.H. (1977) Atmospheric dispersion and transport within coastal regions -- Part I., Tracer study of power plant emissions from the Oxnard Plain. Atmospheric Environment 12, 2089-2100.

Lyons W.A. (1975) Turbulent diffusion and pollutant transport in shoreline environments, Lectures on Air Pollution and Environmental Impact Analyses, ed: D.A. Haugen, Amer. Met. Soc., Boston, Mass., 136-208.

Lyons W.A. and Olsson L.E. (1973) Detailed mesometeorological studies of air pollution dispersion in the Chicago lake breeze. Mon. Wea. Rev. 101, 387-403.

Lyons W.A. and Keen C.S. (1976)) Computed 24-hour trajectories for aerosols and gases in a lake/land breeze circulation cell on the western shore of Lake Michigan, Proc. Sixth Conf. on Weather Forecasting and Analysis, Amer. Met. Soc., Albany, New York, May 10-14, 78-83.

McRae G.J., Shair F.H. and Seinfeld J.H. (1981) Convective downmixing of plumes in a coastal environment, J. Applied Meteorology, (in press).

Neiburger M. (1955) Tracer tests of trajectories computed from observed winds, Tech. Report No. 7, Air Pollution Foundation, Los Angeles, California, 59 pp.

Neiburger M. and Edinger J.G. (1954) Summary report on meteorology of the Los Angeles basin with particular respect to the "smog" problem, Report No. 1, Southern California Air Pollution Foundation, Los Angeles, California, 97 pp.

Neiburger M., Renzetti N.A. and Tice R. (1956) Wind trajectory studies of the movement of polluted air in the Los Angeles basin, Report No. 13, Air Pollution Foundation, Los Angeles, California, 74 pp.

Pack D.H. and Angell J.K. (1963) A preliminary study of air trajectories in the Los Angeles Basin as derived from tetroon flights. Mon. Wea. Rev. 91, 583-604.

Raynor G.S., Michael P., Brown R.M. and SethuRaman S. (1975) Studies of atmospheric diffusion from a nearshore oceanic site. J. Appl. Met. 14, 1080-1094.

Sackinger, P., Reible, D.D., Shair F.H. (1981) Uncertainty Propagation for Mass Balances Associated with Transport of Atmospheric Pollutants, submitted for publication in J Air Pollut. Control Assoc.

Schacher G.E., Davidson K.L. and Fairall C.W. (1980) Atmospheric marine boundary layer mixing rates in the California coastal region, Naval Post Graduate School Report No. NPS61-80-003, Monterey, California, 115 pp.

Schacher G.E., Fairall C.W., Davidson K.L. and Houlihan T.M. (1978) Experimental investigation of the marine boundary layer in support of air pollution studies in the Los Angeles Air Basin, Naval Post Graduate School Report No. NPS61-78-002. Monterey, California, 257 pp.

Schatzmann M. (1979) An integral model of plume rise. Atmospheric Environment 13 721-731.

Scorer R.S. (1978) Environmental Aerodynamics, Ellis Horwood Ltd., Chichester, U.K., 488 pp.

SethuRaman S. and Raynor G.S. (1980) Comparison of mean wind speeds and turbulence at a coastal site and an offshore location. J. Appl. Met. 19, 15-21.

Taylor J.R. (1962) Normalized air trajectories and associated pollution levels in the Los Angeles basin, Air Quality Report No. 45, Air Pollution Control District, Los Angeles, California, 135 pp.

Vaughan L.M. and Stankunas A.R. (1974) Field study of air pollution transport in the South Coast Air Basin. Tech. Report No. 197. Metronics Associates, Inc., Palo Alto, California, 135 pp.

TABLE 1

Description of the Coastline Segments that form the Control Surface for SF_6 Mass Balance Calculations

	COASTLINE SEGMENT	TOPOGRAPHIC FEATURES	WIND STATION(S) USED TO CALCULATE AIR FLOW ACROSS COAST	SF_6 MONITORING SITES ALONG THAT SEGMENT OF COASTLINE
1.	Ventura to Pt. Mugu	Coastal Plain	Average of Ventura and Pt. Mugu	Stations 1 through 5
2.	Pt. Mugu to Pt. Dume	Coastal Mountains	Zuma Beach	Stations 6 and 7
3.	Pt. Dume to Pacific Palasades	Coastal Mountains	Malibu	Stations 8 through 10
4.	Pacific Palasades to Redondo Beach	Coastal Plain	Average of Venice and Redondo Beach	Stations 11 through 16
5.	Redondo Beach to Long Beach	Coastal Mountains	Average of Redondo Beach and Long Beach (APCD Station)	Stations 17 through 19
6.	Long Beach to Los Alamitos	Coastal Plain	Average of Long Beach (APCD Station) and Long Beach Airport	Stations 20 through 22
7.	Los Alamitos to Newport Beach	Coastal Plain	Average of Los Alamitos and Newport Beach	Stations 24 through 29

Figure Captions

Figure 1 — Southern California showing the monitoring sites used during the tracer experiment.

Figure 2 — SF_6 concentrations observed aboard the Acania, coordinated with the ship's position and possible plume centerline locations: Test 1.

Figure 3 — Hourly average SF_6 concentrations measured at the coastline during Test 1.

Figure 4a — Material balance on SF_6 release and return: Test 1.

Figure 4b — Material balance on SF_6 release and return during Test 2, computed using mixing depths implied by the location of the sub-tropical inversion base.

Figure 5 — SF_6 concentrations observed aboard the Acania, coordinated with the ship's position and possible plume centerline locations: Test 2.

Figure 6 — Hourly average SF_6 concentrations measured at the coastline during Test 2.

Figure 7 — Retention time distribution for tracer material within the marine environment. Symbols indicate time measured from the midpoint of the tracer release. Error bounds indicate the 5 hour span during which the returning tracer might have been released.

Figure 8 — SF_6 dosage (ppt-hr) observed along the coastline per g-mole of SF_6 released during Tests 1 and 2.

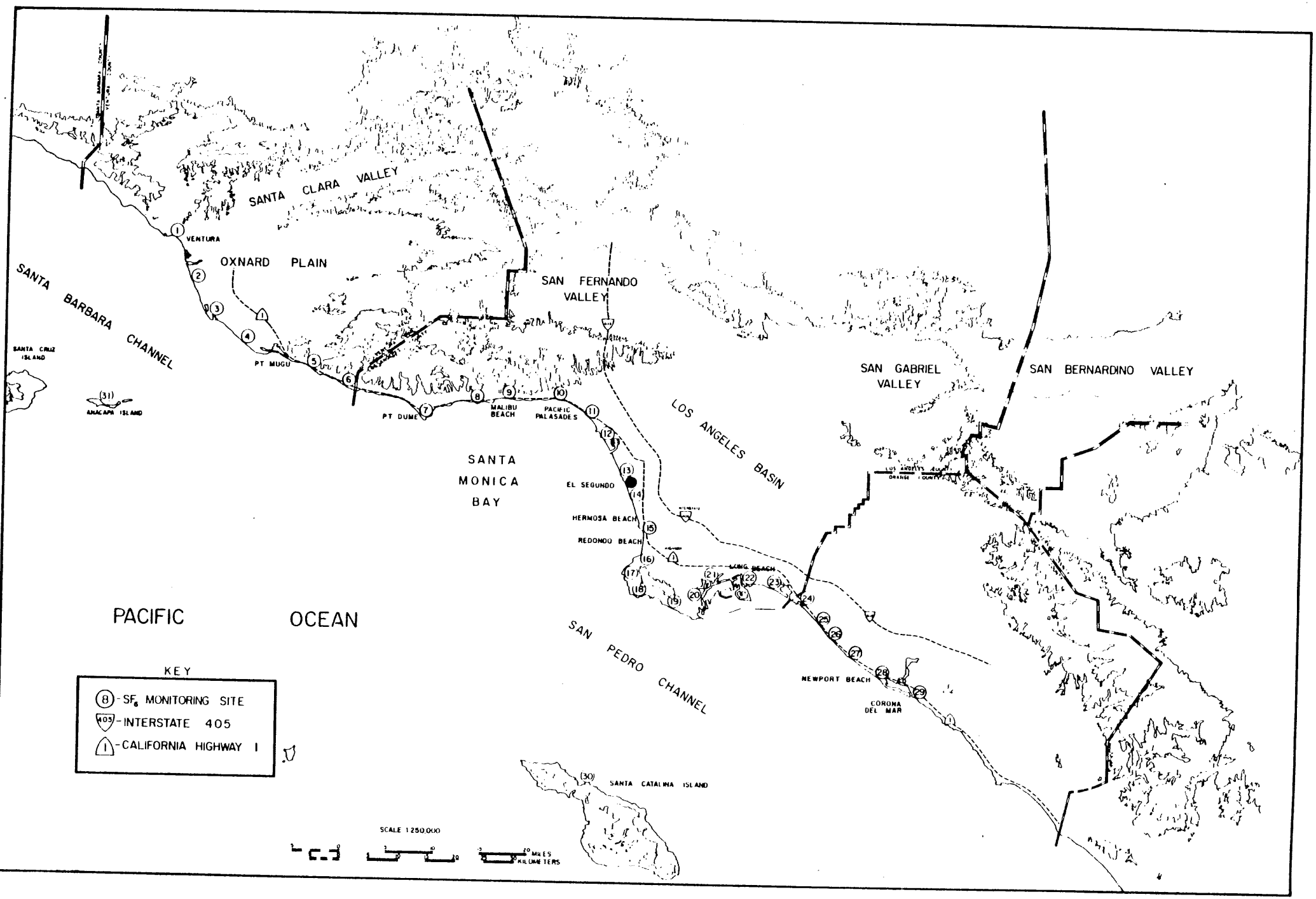
SANTA CLARA VALLEY
VENTURA
OXNARD PLAIN
SANTA BARBARA CHANNEL
SAN FERNANDO VALLEY
SANTA CRUZ ISLAND
ANACAPA ISLAND
PT MUGU
PT DUME
MALIBU BEACH
PACIFIC PALASADES
SAN GABRIEL VALLEY
SAN BERNARDINO VALLEY
LOS ANGELES BASIN
SANTA MONICA BAY
EL SEGUNDO
HERMOSA BEACH
REDONDO BEACH
LONG BEACH
NEWPORT BEACH
CORONA DEL MAR
PACIFIC OCEAN
SAN PEDRO CHANNEL
SANTA CATALINA ISLAND
KEY
8 - SF6 MONITORING SITE
405 - INTERSTATE 405
1 - CALIFORNIA HIGHWAY 1
SCALE 1:250,000
MILES
KILOMETERS

FIGURE 1

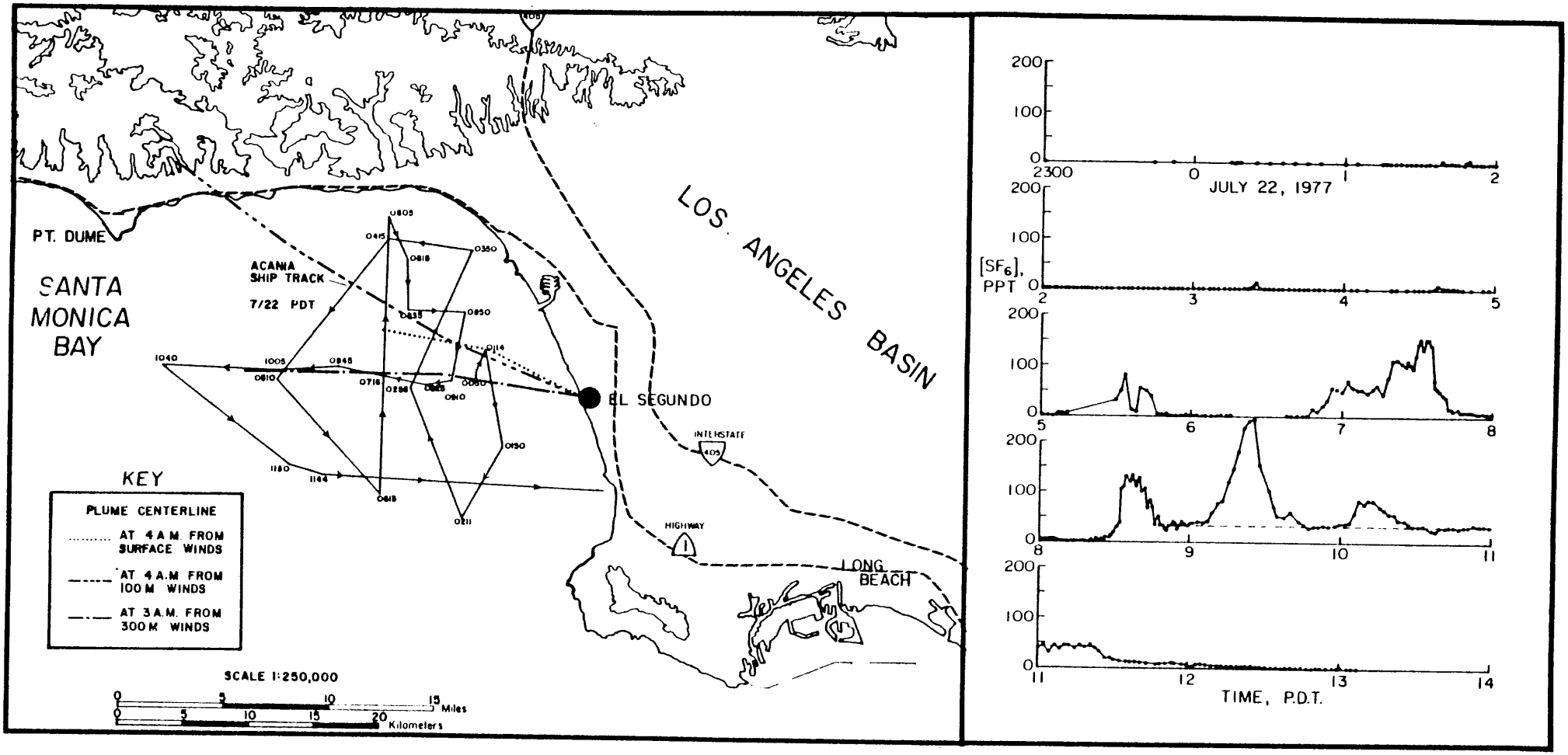
PT. DUME
SANTA MONICA BAY
ACANIA SHIP TRACK
7/22 PDT
LOS ANGELES BASIN
EL SEGUNDO
INTERSTATE
405
HIGHWAY
1
LONG BEACH
KEY
PLUME CENTERLINE
..... AT 4 A.M. FROM SURFACE WINDS
----- AT 4 A.M. FROM 100 M WINDS
—·— AT 3 A.M. FROM 300 M WINDS
SCALE 1:250,000
0 5 10 15 Miles
0 5 10 15 20 Kilometers
JULY 22, 1977
[SF6], PPT
TIME, P.D.T.

FIGURE 2

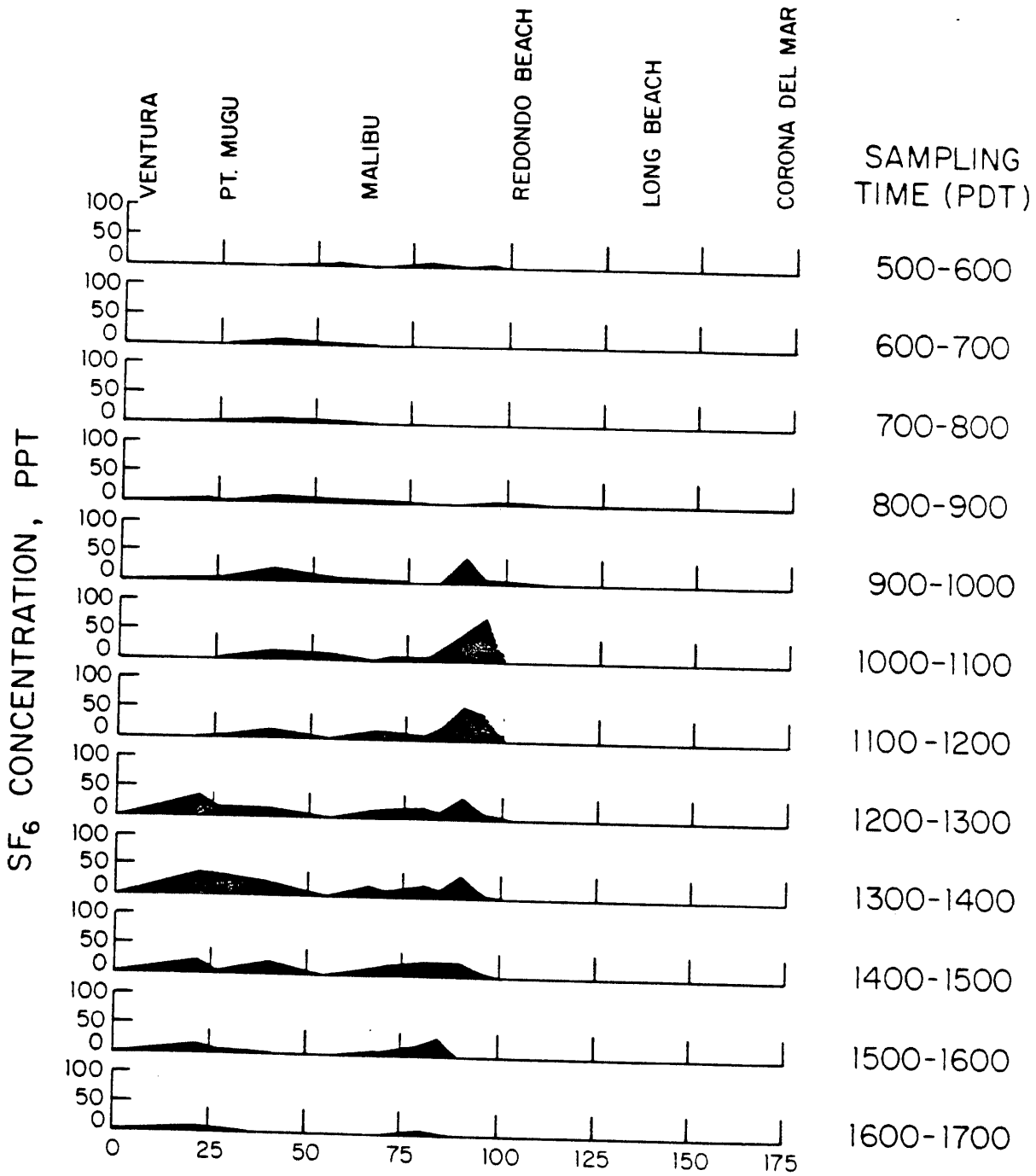
VENTURA
PT. MUGU
MALIBU
REDONDO BEACH
LONG BEACH
CORONA DEL MAR
SAMPLING TIME (PDT)
500-600
600-700
700-800
800-900
900-1000
1000-1100
1100-1200
1200-1300
1300-1400
1400-1500
1500-1600
1600-1700
100
50
0
SF_6 CONCENTRATION, PPT
0
25
50
75
100
125
150
175
DISTANCE SOUTH ALONG COAST, FROM VENTURA (KM)
TEST NO. 1 CONDUCTED ON 7-22-77

FIGURE 3

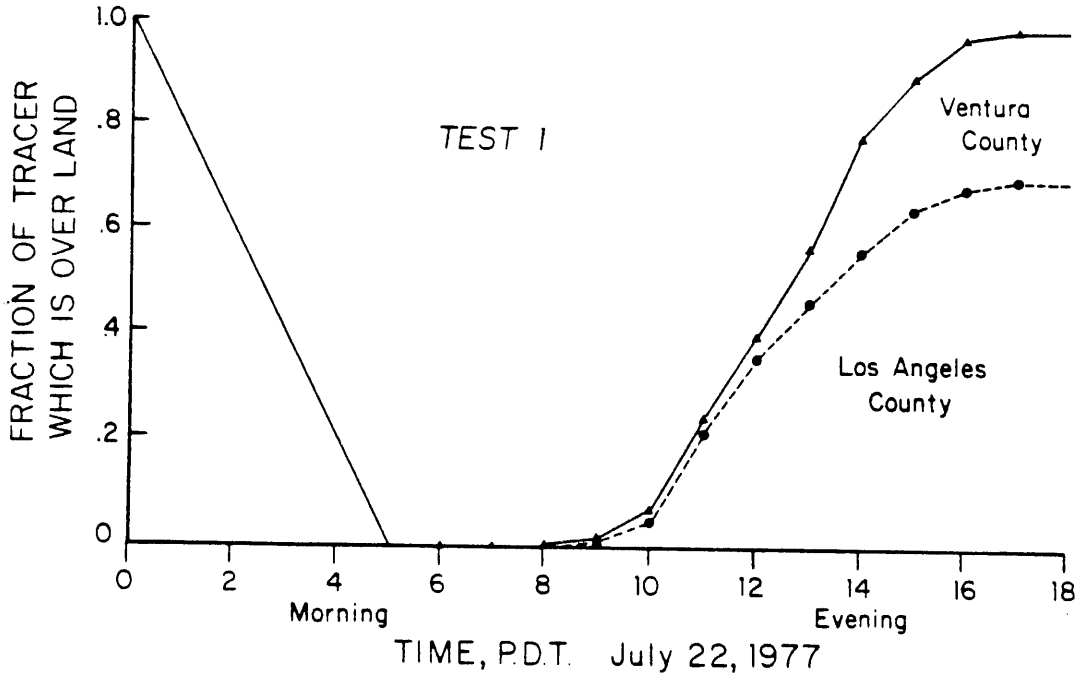

FIGURE 4a

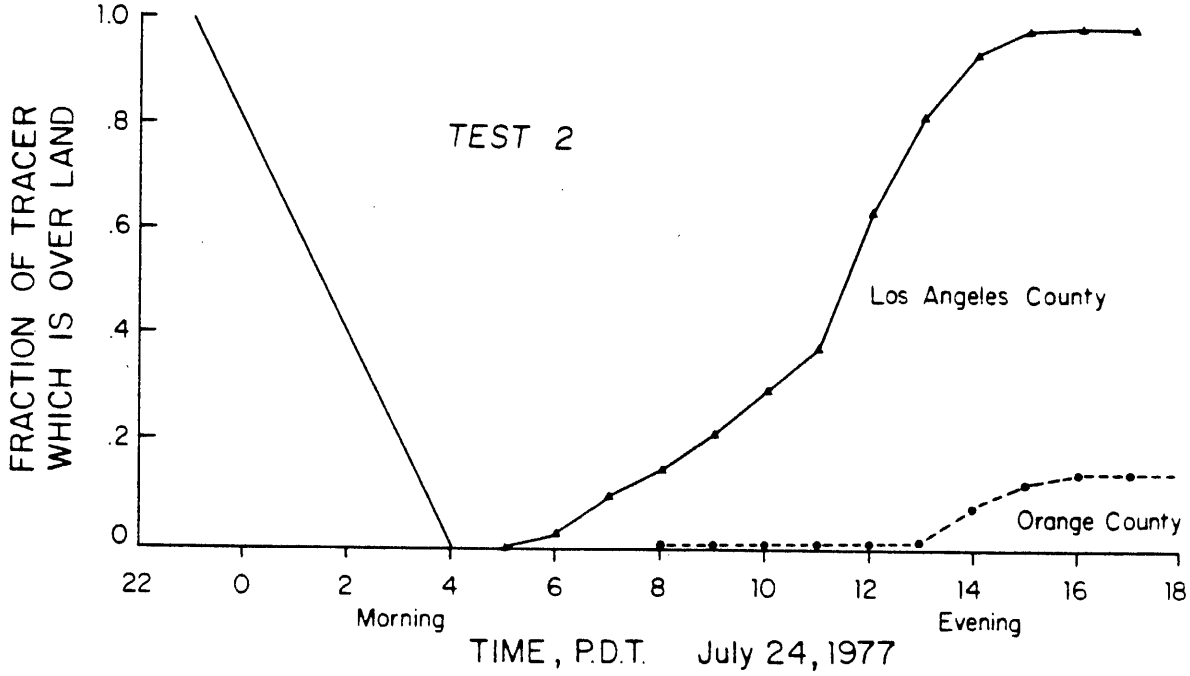

FIGURE 4b

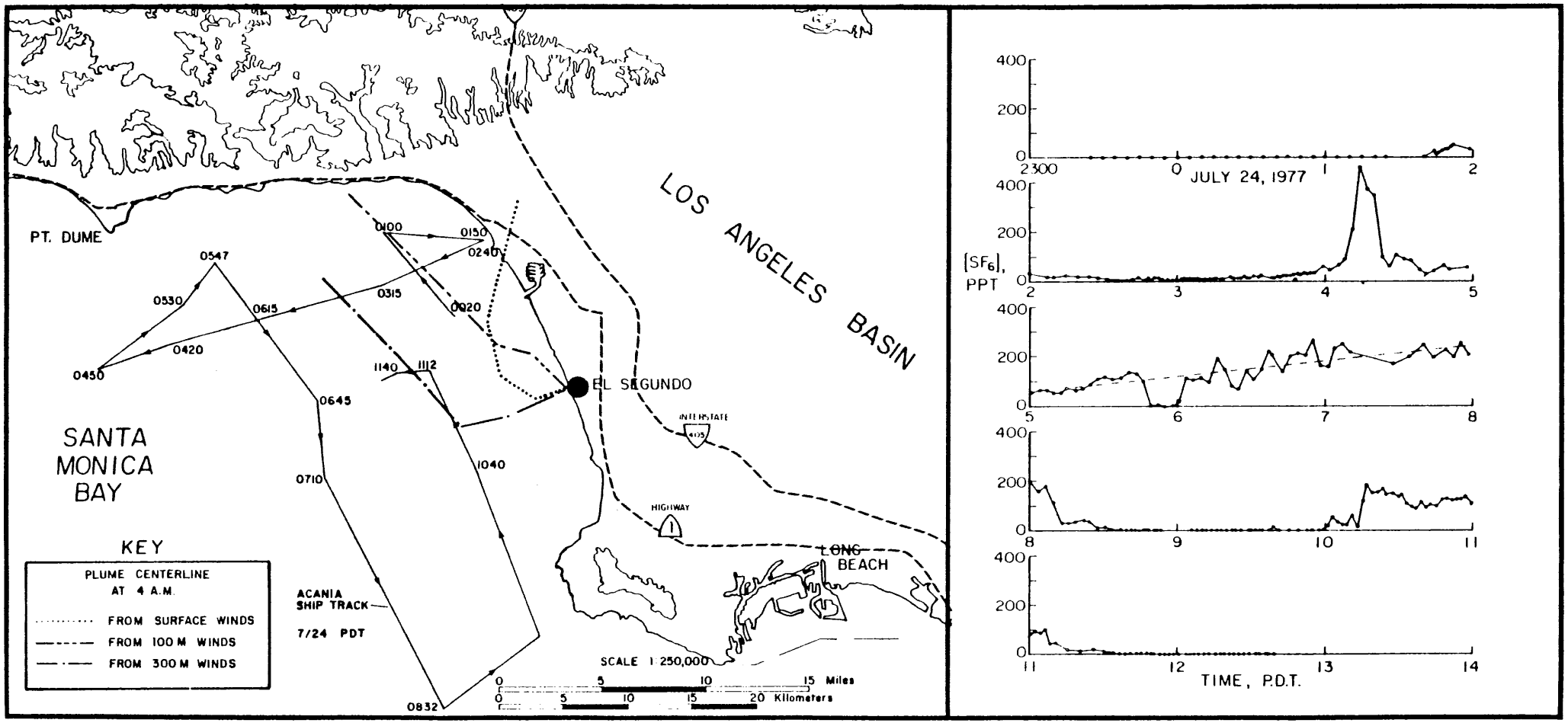
PT. DUME
0547
0530
0615
0420
0450
0100
0150
0240
0315
0020
1140
1112
0645
0710
1040
0832
EL SEGUNDO
LOS ANGELES BASIN
SANTA MONICA BAY
INTERSTATE
HIGHWAY
LONG BEACH
KEY
PLUME CENTERLINE AT 4 A.M.
FROM SURFACE WINDS
FROM 100 M WINDS
FROM 300 M WINDS
ACANIA SHIP TRACK
7/24 PDT
SCALE 1:250,000
0 5 10 15 Miles
0 5 10 15 20 Kilometers
400
200
0
2300
0
1
2
JULY 24, 1977
[SF6], PPT
2
3
4
5
5
6
7
8
8
9
10
11
11
12
13
14
TIME, P.D.T.

FIGURE 5

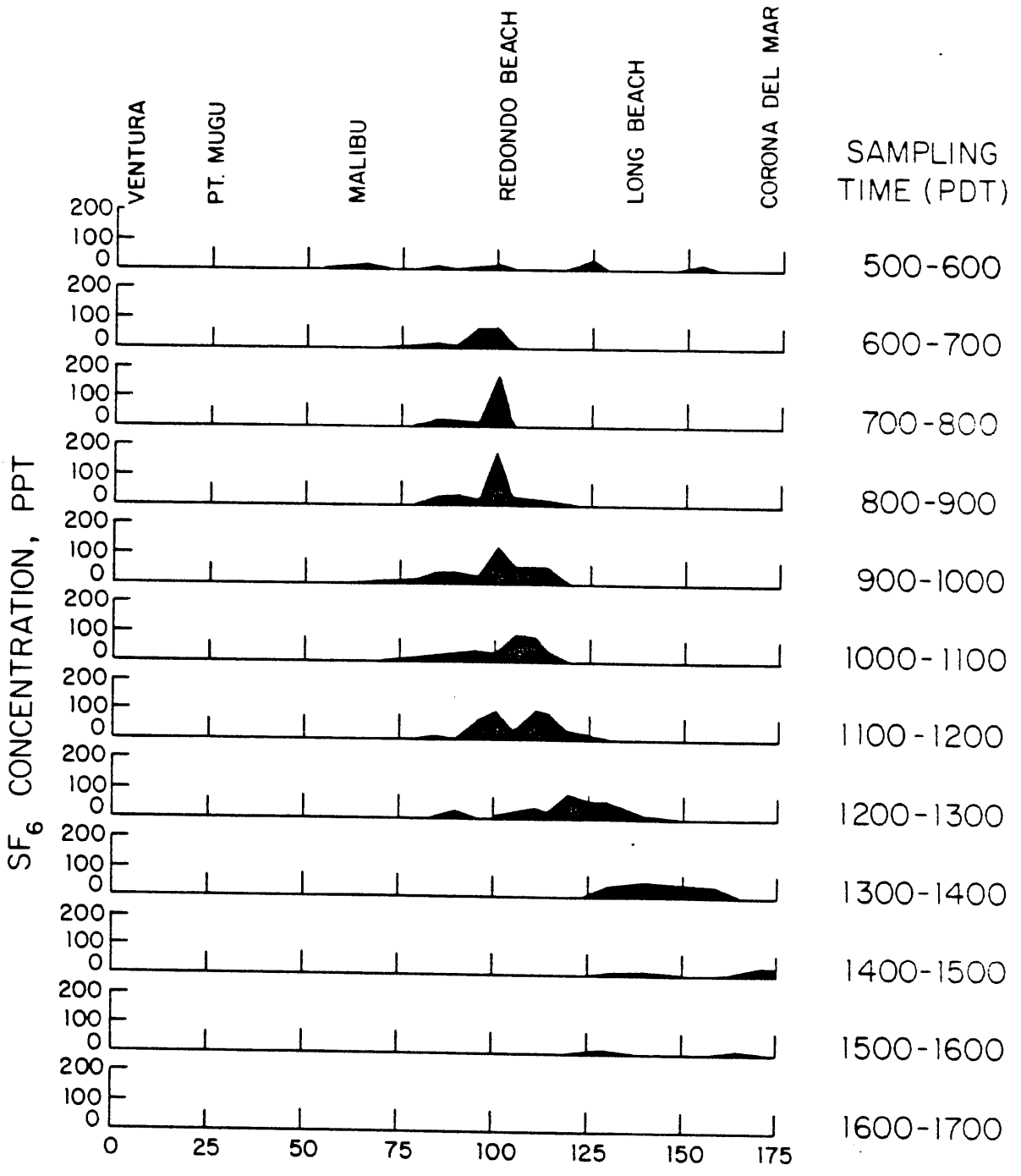
VENTURA
PT. MUGU
MALIBU
REDONDO BEACH
LONG BEACH
CORONA DEL MAR
SAMPLING TIME (PDT)
500-600
600-700
700-800
800-900
900-1000
1000-1100
1100-1200
1200-1300
1300-1400
1400-1500
1500-1600
1600-1700
200
100
0
SF_6 CONCENTRATION, PPT
0
25
50
75
100
125
150
175
DISTANCE SOUTH ALONG COAST, FROM VENTURA (KM)
TEST NO. 2 CONDUCTED ON 7-24-77

FIGURE 6

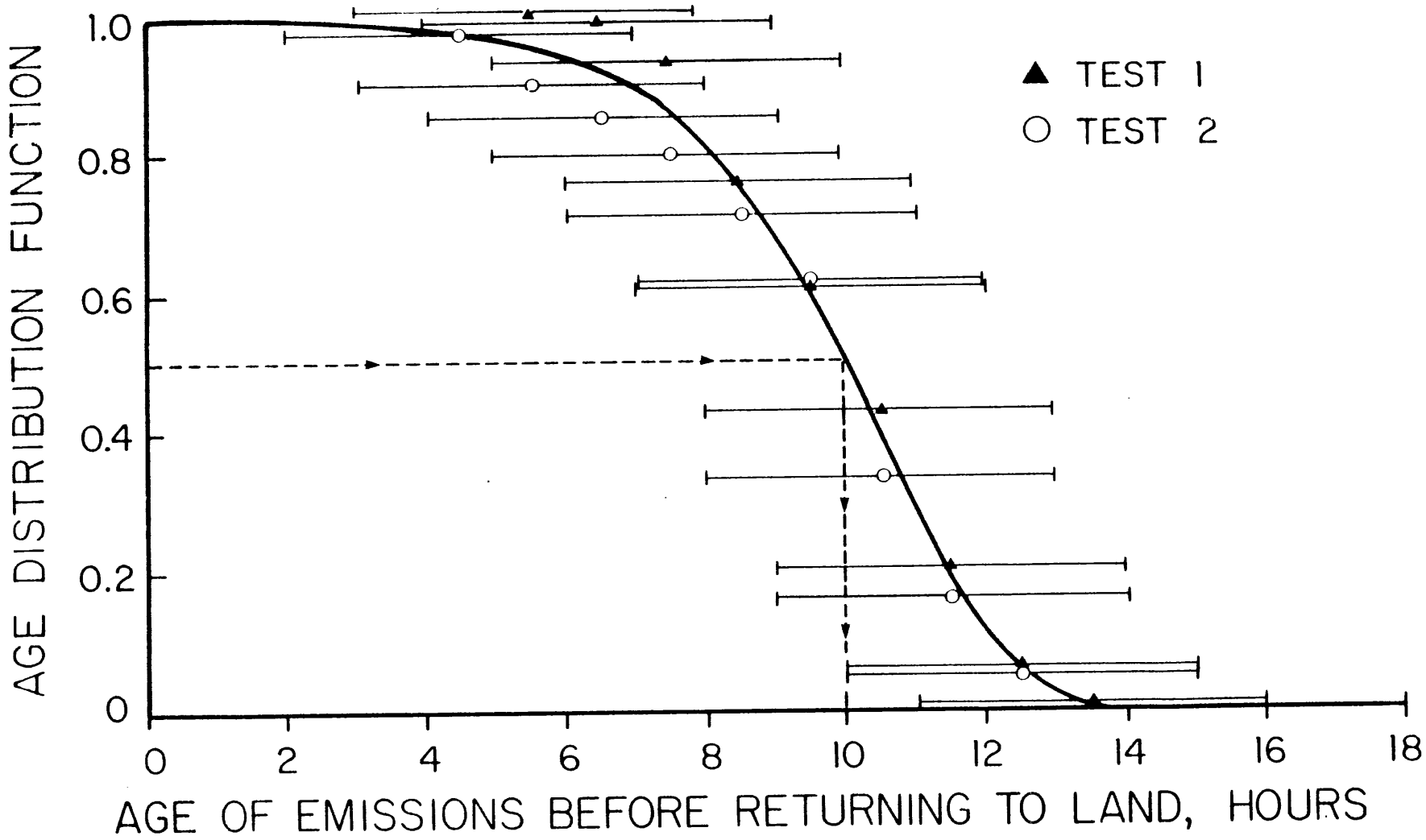
AGE DISTRIBUTION FUNCTION
1.0
0.8
0.6
0.4
0.2
0
0
2
4
6
8
10
12
14
16
18
AGE OF EMISSIONS BEFORE RETURNING TO LAND, HOURS
TEST 1
TEST 2

FIGURE 7

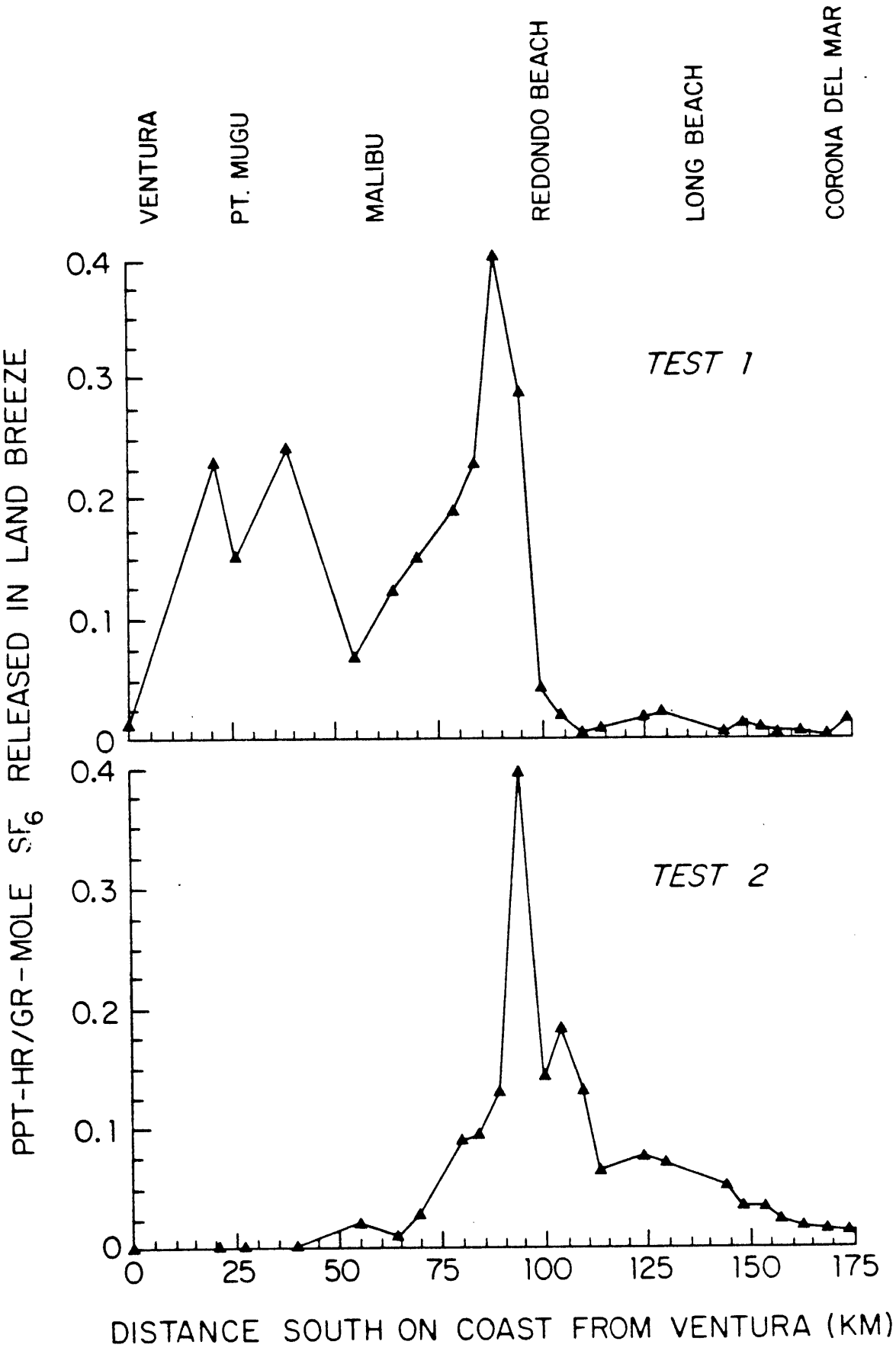
VENTURA
PT. MUGU
MALIBU
REDONDO BEACH
LONG BEACH
CORONA DEL MAR
TEST 1
TEST 2
PPT-HR/GR-MOLE SF_6 RELEASED IN LAND BREEZE
0.4
0.3
0.2
0.1
0
0
25
50
75
100
125
150
175
DISTANCE SOUTH ON COAST FROM VENTURA (KM)

FIGURE 8

Chapter 2

CONVECTIVE DOWNMIXING OF PLUMES IN A COASTAL ENVIRONMENT

Gregory J. McRae
Fredrick H. Shair†
John H. Seinfeld†

Environmental Quality Laboratory
California Institute of Technology
Pasadena, California 91125

July 1981

In press, J. Applied Meteorology

J. Applied Meteorology
(in press)
24 July 1981

CONVECTIVE DOWNMIXING OF PLUMES IN A COASTAL ENVIRONMENT

Gregory J. McRae
Fredrick H. Shair[†]
John H. Seinfeld[†]

Environmental Quality Laboratory
California Institute of Technology
Pasadena, California 91125

ABSTRACT

This paper describes the results of an atmospheric tracer study in which sulfur hexafluoride (SF_6) was used to investigate the transport and dispersion of effluent from a power plant located in a coastal environment. The field study demonstrated that material emitted into an elevated stable layer at night can be transported out over the ocean, fumigated to the surface, and then be returned at ground level by the seabreeze on the next day. At night when cool stable air from the land encounters the warmer ocean convective mixing erodes the stable layer forming an internal boundary layer. When the growing boundary layer encounters an elevated plume the pollutant material, entrained at the top of the mixed layer, can be rapidly transported $\sim$ 20 minutes to the surface. Various expressions for the characteristic downmixing time ($\lambda = Z_i/w_*$) are developed utilizing the gradient Richardson Number, the Monin-Obukhov length and turbulence intensities. Calculations using these expressions and the field data are compared with similar studies of convective mixing over the land.

[†]Department of Chemical Engineering

Introduction

A major influence on pollutant dispersion and transport in coastal environments is the presence of land/sea breeze circulation systems. Unfortunately the characterization of turbulent transport is complicated by the presence of flow reversals and differing atmospheric stabilities. Since many large sources are located in shore line environments it is important to understand the mixing characteristics within the boundary layer. A field experiment designed to determine the fate of pollutants emitted into the offshore flow associated with a land/sea breeze circulation system, was carried out by Shair et al. (1981). In that study it was found that tracer material emitted into an elevated stable layer at night could be transported out over the ocean, fumigated to the surface, and then be returned at ground level by the sea breeze on the next day. The objectives of this work are to examine the vertical transport processes responsible for this rapid downmixing and to characterize the mixing rates within the internal boundary layer formed when cool air from the land is advected out over a warm ocean surface.

Description of Field Experiment

Because of the complexity of atmospheric flows, the only direct way to relate the emissions from a particular source to observed concentrations is to tag the source exhaust gases so they can be uniquely identified. Over the last few years a variety of atmospheric tracers, including sulfur hexafluoride (SF_6), fluorescent particles, halocarbons and deuterated methane, have been used in transport and diffusion studies. Sulfur hexafluoride was used in this experiment because it is gaseous, physiologically inert, chemically stable and easily detected using electron-capture gas chromatography (Simmonds et al. 1972). Drivas and Shair (1974), Lamb et al. (1978ab) and Dietz and Cote (1973)

have successfully demonstrated the utility of SF_6 as a tracer in large scale field studies. Current analysis techniques have achieved detection limits of $2x10^{-13}$ parts SF_6 per part of air. From a practical point of view both the release techniques and sampling protocols are well established and reliable.

Each experiment was carried out by injecting the tracer gas into the number 4 stack of the Southern California Edison El Segundo power plant located on the shore of Santa Monica Bay (Figure 1). This particular chimney is 61m high and 4.3m in diameter. The tracer was released at a time when the flow, at the effective stack height, was offshore. Before each experiment an initial estimate of the plume rise was determined using Briggs' formulae (Briggs, 1969; 1975) for neutral conditions. For the particular load conditions (0.57 of capacity), an exhaust gas temperature of 365 ^{o}K and a gas flow rate of 230 m^3/s the plume rise was estimated to be 250m. This information, together with the vertical wind distribution obtained from pibal releases, was used to establish the time to initate the tracer injection so that the material was released into the offshore flow. After the experiment a more detailed calculation, accounting for the actual vertical variations in wind and temperature profiles, was carried out using the Schatzmann (1979) integral plume rise model, using meteorological data from Schacher et al. (1978). During the first test, on 22 July 1977, 90 kg of SF_6 was released at a rate of 5.0 g/s from 00:05-05:00 PDT. During the second test 245 kg of SF_6 were released, at a higher rate of 13.6 g/s, from 23:03 on 23 July 1977 until 04:00 on July 24.

The amount and release rates for each experiment were selected so that there was sufficient material to distinguish the source from the background at the maximum sampling distance. If the total amount of tracer released during each experiment were to be uniformly distributed throughout a volume of

1600 km^2 x 300m(i.e. the area of Santa Monica Bay times the estimated plume rise above the ocean surface) then the average tracer concentration would have been 50 ppt a value well above both the detection limit and normal background levels. Most of the current world background concentration of <0.5 ppt is a result of leakages from high-voltage power transformers and switching systems where SF_6 is used for corona discharge suppression.

Hourly averaged air samples were collected continuously, from 05:00-17:00 PDT during each of the test days, at 29 coastal sites located from Ventura to Corona del Mar (Figures 1 and 2). This was to observe the tracer flux across the coast during the sea breeze on the day following the nighttime release. Subsequent mass balance calculations using these measurements were able to account for virtually 100% of the material released during both experiments (Shair et al. 1981). Samples were analyzed using the methodology described in Lamb et al. (1978ab). In addition, grab samples were collected every five minutes on board a ship traversing Santa Monica Bay and analyzed using portable electron-capture gas chromatographs. This sampling protocol provided rapid feedback on the tracer concentrations and plume position during each experiment. The measurements taken on board the ship are shown in Figures 1 and 2. Sampling on board the ship was started one hour before each release so that any possible background levels could be detected. All samples were collected in 300 cm^3 plastic syringes and were analyzed within one day of each experiment. At the coastal monitoring sites battery-powered sequential samplers were used to determined the hourly averaged SF_6 concentration levels. In addition automobile sampling traverses were conducted periodically along coastal highways between 10:00-14:27 hours PDT on July 22 and between 02:35-15:40 on July 24. Grab samples were collected at 0.8 to 3.2 km intervals along the coastal highway between Redondo Beach and Malibu.

The results from the shore measurements and automobile traverses were used by Shair et al. (1981) to calculate the flux of SF_6 across the coast.

The tracer experiments were carried out in collaboration with investigators from the Environmental Physics Group at the Naval Post-graduate School in Monterey, California. The research vessel Arcania was used as a platform to collect meteorological data in the vicinity of Santa Monica Bay. The ship was equipped with a complete suite of meteoroloigcal equipment capable of multi-level measurements (4.2, 7.0 and 22.5 m above the ocean) of mean and fluctuating quantities. Since complete details of the instrumentation can be found in Houlihan et al. (178) and Schacher et al. (1978), the material will not be repeated here. For the particular study of the mixing rates over the ocean, measurements were made of: sea surface temperature T_s, air temperature T_a, humidity/dew point T_d, true wind speed u, direction θ, and temperature inversion height Z_i. The wind direction θ, is particularly useful since it can be used to differentiate local (land and sea breeze) circulations. Both the wind speed and direction have been corrected to account for the ship motion. In addition, during the period 19-26 July, 14 radiosondes were released to examine the vertical temperature structure. During each tracer experiment pibals were released each hour at a site close to the release point so that the horizontal winds as a function of elevation could be determined. Observations made at the 100 and 300 m levels were used to calculate plume trajectories from the release point. Some of these results are superimposed on Figures 1 and 2. The complete data sets describing the meteorological conditions are contained in the reports by Schacher et al. (1978, 1980). For convenience a summary of key information from these sources, together with the calculated virtual heat flux Q_o, is presented in Table 1.

Since the pattern of results observed on board R/V Arcania on both days were similar it suffices to discuss the experiment conducted on 22 July. A more detailed discussion of the concentration levels measured at the coastal monitoring stations is contained in Shair et al. (1981). Prior to 5:30 PDT, when the mixing depth was below 200 m, the ship passed under the calculated plume positions at 1:00, 3:25 and 4:38 PDT and no significant concentrations of SF_6 were observed. At 5:30 PDT, when the ship was 6.4 km south of the plume, the first significant peak (80 ppt) was recorded at a time when the mixed layer was growing above the 200 m level. From 6:00 PDT onwards all the concentration peaks at 7:30, 8:35 and 9:25 were observed when the ship was in the vicinity of the plume and the mixed layer height was above 200 m. From 8:30 to 11:30 PDT the SF_6 exceeded 20 ppt and the ship was always within 3 km of the plume. Lower concentrations were observed when the ship and the plume separation increased to more than 15 km. The only major difference between the two tests was the increased wind speeds and mixing heights on 23-24 July. While this, together with the wind shear, enhanced the horizontal dispersion of SF_6 there were no significant differences in the observed vertical mixing rates.

Although the power plant effluent was emitted well above the surface into an elevated stable layer where vertical mixing could be expected to be quite small, large amounts of tracer suddenly appeared at the sampling sites close to the ocean surface. The remaining sections of this work are devoted to a discussion of the reasons for the rapid transport of tracer material to the surface.

Vertical Mixing Over the Ocean

The problem of dispersion and transport near coastlines and large lakes has received considerable attention in the literature. [See for example Lyons (1975), Businger (1975), Misra (1980), Raynor et al. (1980) and Orgill (1981).] The purpose of this section is to examine the results from prior observations applicable to the present field experiment, since few, if any, studies have been made of convective activity over the ocean at night. Since the ocean temperatures during the experiments were greater than that of the air, it can be seen that the conditions are similar to those observed over the land during the day time.

Under the action of buoyancy forces induced by surface heating, parcels of warm air, displaced by mechanical turbulence, rise all the way through the mixed layer and impinge at the inversion base. To compensate for these vertical motions, zones of sinking air fill the spaces between rising air parcels. Close to the top of the mixed layer the net flux is directed downward. Adiabatic transport of air through the capping inversion would produce the negative flux, which in turn suggests a mechanism for substantial entrainment of air and tracer material into the mixed layer from above (Ball, 1960; Kaimal et al., 1976 and

Deardorff et al. 1980). The regions of upward flux are obviously thermals which originate near the surface shear layer and so the transport is occurring over a scale Z_i.

The shape of the updraft regions in the thermals resemble the three-dimensional convection patterns observed by Frisch et al. (1975) with dual-Doppler radar. Kaimal et al. (1976) suggested that the rising air spreads out laterally as it reaches the inversion base, producing a dome-like depression at the interface, and returns as a down draft along the "side wall" of the thermal. These structures can be observed with acoustic sounders and radars. Arnold et al. (1975) found that dome-like structures are co-located with the thermals detected simultaneously by an acoustic sounder. The strong returns from the side walls indicate the presence of entrained air from the inversion. The inverted U structures in the vertical section and the doughnut-shaped patterns in plan views observed by Hardy and Ottersten (1969), Konrad (1969), Arnold and Rowland (1976) and Agee et al. (1973) in radar returns indicate the presence of convective cells.

Arnold and Rowland (1976) conclude that most of the entrainment takes place along the top of the dome. Here either the Kelvin-Helmholtz instability or wave-like overturning of the dome structures could provide the mechanism for entrainment. This process is illustrated in Figure 3 where the tops of the convective cells can rise to the elevation of the SF_6. Entrainment of this material and its subsequent transport to the surface lead to the large concentration increases. Areas of low concentration would then result when the ship went beyond the bounds of the cloud or when the convective cells did not reach the height of the tracer. A detailed examination of the mechanism of entrainment and mixed layer growth is beyond the scope of this work and

for details the reader is referred to Stull (1973), Venkatram (1976), Zeman and Tennekes (1977), Heidt (1977) and Deardorff (1978). Convective entrainment has been studied in the laboratory by Willis and Deardorff (1976a), Manins (1977) and Deardorff et al. (1980). The characteristic separation distance of the thermals given by Kaimal et al. (1976) is 1.3 to 1.4 Z_i with a diameter to depth ratio for the Rayleigh cells being of the order 40:1 (Agee and Chen, 1973).

With this background it is now possible to advance an explanation of the findings from the tracer experiments. When the cool stable air from the land encounters the warmer ocean surface, convective mixing begins to erode the overlying stable layer forming an internal boundary layer (Figure 4). (The growth of this layer as a function of distance from the shore can be seen in the acoustic sounder traces.) Convective mixing in the surface layer entrains air from the stable layer aloft causing the inversion base to rise from the surface. Heating of the mixed layer is due to the combined effects of an upward heat flux from the ocean and a downward flux from the warmer air in the inversion. Continued growth of the mixed layer ultimately leads to a situation where the internal boundary layer intercepts the elevated plume and the tracer material. Since below the inversion base the mixing is rapid, the entrained SF_6 is quickly transported to the surface. Except for the strength of the convective mixing, the conditions of the experiment are similar to those that occur over the land during the day. Subsequent sections of this work are devoted to an estimate of the rate at which the tracer material is transported to the surface.

Mixing Times Under Convective Conditions

Under convective conditions a variety of interacting processes are involved in the mixing within the boundary layer. The relative role of buoyancy $\overline{w'T_v'}$, in comparison with the transfer of energy from the mean motion $\overline{u'w'}\partial u/\partial z$, can be expressed in terms of the flux Richardson Number R_f (Monin and Yaglom, 1971; Kraus, 1972),

$$R_f = \frac{\frac{g}{\bar{T}}\overline{T_v'w'}}{\overline{u'w'}\frac{\partial u}{\partial z}} \tag{1}$$

where T_v is the virtual temperature. A more commonly used expression is the gradient Richardson Number R_i

$$R_i = \frac{g\left(\frac{\partial \bar{T}_v}{\partial z} + \Gamma\right)}{T_v\left(\frac{\partial \bar{u}}{\partial z}\right)^2} = \frac{g}{\theta_v}\,\frac{\frac{\partial \bar{\theta}_v}{\partial z}}{\left(\frac{\partial \bar{u}}{\partial z}\right)^2} = \frac{N^2}{\left(\frac{\partial \bar{u}}{\partial z}\right)^2} \tag{2}$$

where N is the Brunt-Väisälä frequency, θ_v the potential temperature, and Γ the adiabatic lapse rate. The relationship between R_f and the more easily measured Richardson number R_i is simply $R_f = \alpha R_i$ where α is the ratio of the turbulent eddy diffusion coefficients for heat and momentum. Under a spatial homogeneity assumption temporal changes in the total mean kinetic energy are negligible if synoptic and mesoscale forces driving the boundary layer vary slowly (Caughey et al. 1978). In particular, if the time scales for the large scale processes are long compared to the time required for the boundary layer to adjust then the rate of change of turbulent kinetic energy per unit mass is negligible. If the contribution from the flux divergence term in the energy equation is small, then, with the above assumptions, the turbulent kinetic energy equation reduces to

$$- \overline{u'w'} \frac{\partial u}{\partial z} (1 - R_f) - \varepsilon = 0 \qquad (3)$$

where ε is the dissipation or the rate of conversion of kinetic into internal energy by the viscous forces in the smallest eddies. Since $\varepsilon > 0$ and $-\overline{u'w'}\partial u/\partial z$ is practically always greater than zero, stationary, undamped turbulence is possible only if $R_f < 1$. This result is often used as an approximate criterion for defining the transition to turbulence in a stratified medium. For the purpose of analyzing the experimental results within this framework it is useful to identify the appropriate length and velocity scales. A key scaling parameter is the Monin-Obukhov length L defined by

$$\frac{1}{L} = - \frac{kgQ_o}{u_*^3 T} = - \frac{kg}{u_*^3 T} \left[Q + 0.61 \frac{TM_o}{\rho} \right] = \frac{1}{L_T} + \frac{1}{L_q} \qquad (4)$$

where $Q_o = (\overline{T_v'w'})_o$ is the virtual surface heat flux that accounts for the influence of humidity fluctuations on buoyancy, k the von Karman constant, $u_*^2 = - \overline{u'w'}$ the friction velocity, L_T and L_q are the Monin-Obukhov lengths calculated from the surface heat and evaporative fluxes. Physically L is the height at which the two production terms are approximately of equal magnitude.
One of the major differences in examining conditions over the ocean or other large bodies of water is that the density stratification is controlled not only by the surface heat flux but also by the water vapor flux. The measurements made by McBean and MacPherson (1975) over Lake Ontario indicate that there can be a significant difference between L_q and L_T, that in turn have a major influence on L.

Above the surface layer a more appropriate length scale for the eddies is the mixed layer depth Z_i. While there is some controversy associated with a formal definition of Z_i, in this work it is defined as the elevation of the

lowest inversion base. The studies of Deardorff (1972) and Deardorff et al. (1980) indicate that this is an appropriate boundary layer height for momentum and heat. Under convective conditions the appropriate velocity scale, above the surface layer, is given by

$$w_* = \left[\frac{g}{\bar{T}} Z_i Q_o\right]^{\frac{1}{3}} = \left[\frac{g}{\bar{T}} Z_i \left(\overline{w'T'}\right)_o\right]^{\frac{1}{3}} = \left(-\frac{1}{k}\frac{Z_i}{L}\right)^{\frac{1}{3}} u_* \qquad (5)$$

The characteristic time scale under convective conditions is then given by $\lambda = Z_i/w_*$. Willis and Deardorff (1976b) have shown that material released instantaneously at the surface becomes nearly well mixed within a travel time of approximately 3λ. In the field experiment the tracer material was "released" at the top of the mixed layer. Apart from the small contribution due to mechanical mixing the characteristic mixing time can be expected to be similar to that for a surface release. The reason for this is that the effective aerodynamic roughness of the ocean is very small.

There are a variety of means of estimating the fluxes needed to evaluate the above expressions. Three of the more common techniques are: the profile or gradient method, the variance budget or dissipation technique, and bulk aerodynamic calculations using air-sea differences. Schacher et al. (1978, 1980) employed the latter approach in reducing the meteorological data from the field experiment. A detailed discussion of these and other procedures is presented in Busch (1977). The key results from Schacher et al. (1978, 1980) are summarized in Table 2. In particular the frequency distribution of convecting mixing times observed during the period 19-23 July is shown in Figure 5 together with a similar distribution for daytime conditions over the land. The characteristic mixing times for both experiments were very similar. The influence of a much larger surface heat flux during the day is readily apparent.

In the surface layer, the velocity distribution can be expressed in terms of Monin-Obukhov similarity theory,

$$\frac{\partial \bar{u}}{\partial z} = \frac{u_*}{kz}\,\phi_m\,(\frac{z}{L}) \tag{6}$$

where ϕ_m is an experimentally determined function that corrects for the effects of buoyancy on turbulence. Businger et al. (1971) have constructed expressions for momentum ϕ_m and heat ϕ_h from an analysis of field data. For unstable conditions $z/L < 0$ the formulae are given by

$$\phi_m\,(\frac{z}{L}) = \left[1 - 15(\frac{z}{L})\right]^{-\frac{1}{4}} \tag{7}$$

$$\phi_h^2(\frac{z}{L}) = \phi_m(\frac{z}{L}) \tag{8}$$

These results, together with (3), the definition of u_* and the relation $R_i = \alpha R_f$ can combined to give

$$u_*^3 = \frac{kz}{(1-\alpha R_i)\phi_m(\frac{z}{L})} \tag{9}$$

The characteristic mixing time τ_m, can be defined in terms of the convective time scale λ as $\tau_m = 3\lambda = 3Z_i/w_*$. Using (5), and the expression $\phi_m R_f = z/L$, (9) can be manipulated to give an estimate of the mixing time in terms of the measured dissipation rate and gradient Richardson number R_i

$$\tau_m = 3\left[\frac{Z_i^2}{\varepsilon}\left(1 - \frac{1}{\alpha R_i}\right)\right]^{\frac{1}{3}} \tag{10}$$

For near neutral conditions, Businger et al. (1971) determined that $\alpha = 1.35$ and so a simple upper bound on (10) is $\tau_m \simeq 3[-Z_i^2/\varepsilon R_i]^{1/3}$. For unstable conditions when $|R_i| >> 1$, a lower bound is given by $\phi_m = 3[Z_i^2/\varepsilon]^{1/3}$. Using the

data tabulated in Appendix B of Schacher et al. (1978) the limits on the convective mixing times can be calculated and are shown in Table 3 for the experiment conducted on 22 July. The important result from the tracer experiments is that the calculated mixing rates using either the bulk or dissipation methods produces results consistent with the observed fumigation times. The rapid concentration increases were measured during times when the ship was beneath the plume and the mixed layer height exceeded 200 m.

Eddy Diffusion Coefficients

A basic problem with modeling convectively driven flows is that the turbulent mixing is no longer described by local concentration gradients. Nevertheless, there are some circumstances in which it is desirable to parameterize the diffusive fluxes by a K-Theory model. The objective of this section is to present a simple formulation that produces transport times consistent with observed fumigation rates. Some recent work by Crane et al. (1977) and McRae et al. (1981) indicates that vertical eddy diffusivity profiles for unstable conditions can be scaled by a single profile of the form

$$K_{zz} = w_* Z_i \; f\left(\frac{z}{Z_i}\right) \tag{11}$$

Lamb et al. (1975) derived an expression for f using the numerical turbulence model of Deardorff (1970). The profile adopted by McRae et al. (1981) is given by

$$\frac{K_{zz}}{w_* Z_i} = \begin{cases} 2.5\, k\left(\frac{z}{Z_i}\right)^{\frac{3}{4}}\left[1 - 15\left(\frac{z}{L}\right)\right]^{\frac{1}{4}} & ; \quad 0 < \frac{z}{Z_i} \leq 0.05 \\ 0.021 + 0.408\left(\frac{z}{Z_i}\right) + 1.352\left(\frac{z}{Z_i}\right)^2 - 4.096\left(\frac{z}{Z_i}\right)^3 + 2.560\left(\frac{z}{Z_i}\right)^4 & ; \quad 0.05 < \frac{z}{Z_i} \leq 0.6 \\ 0.2 \exp\left[6 - 10\left(\frac{z}{Z_i}\right)\right] & ; \quad 0.6 < \frac{z}{Z_i} \leq 1.1 \\ 0.0013 & ; \quad \frac{z}{Z_i} > 1.1 \end{cases} \tag{12}$$

As can be seen from Figure 6 the maximum value of the diffusivity occurs when $z/Z_i \simeq 0.5$ and has a magnitude $\sim 0.21 w_* Z_i$. For typical conditions this corresponds to a diffusion time, defined by Z_i^2/K_{zz}, of $\sim 5Z_i/w_*$ that is quite consistent with the bounds shown in Tables 2 and 3.

Conclusions

There are a number of important findings from the tracer study that are of direct relevance to air pollution studies, first of which is that close to the shoreline different stabilities can exist above the land and water surfaces. Under these conditions atmospheric stability cannot be easily determined in terms of conventional classifications. A second finding is that the presence of convective activity can cause downmixing or fumigation of material that can return the next day as a significant increment to the onshore ground level concentration. The process by which this occurs is as follows. During the night, cool stable air is advected out over the ocean. When this air encounters the warmer ocean surface convective mixing begins to erode the stable layer. Once the internal boundary layer has grown to the height of the plume the tracer material, entrained at the top of the mixed layer, is rapidly fumigated to the surface. The characteristic mixing time, inferred from the concentration records, is consistent with an estimate based on the convective time scale $\lambda = Z_i/w_*$ that, for the conditions of the experiment, was $\sim$ 20 min. understanding of these mixing processes and convective activity over the ocean will improve the ability to predict atmospheric dispersion in coastline environments.

ACKNOWLEDGMENTS

This work was supported by the California Air Resources Board under contracts A5-187-30, A5-046-87 and A7-187-30. The assistance of Gordon Schacher

of the Naval Postgraduate School, who supplied descriptions of data reduction procedures and measurement equipment, and Charles Bennett of the California Air Resources Board is appreciated.

REFERENCES

Agee, E.M. and Chen, T.S. (1973), "A Model for Investigating Eddy Viscosity Effects on Mesoscale Convection," J. Atmospheric Sciences, 30, 180-189.

Arnold, A., Rowland, J.R., Konrad, T.G., Richter, J.H., Jensen, D.R. and Noonkester, V.R. (1975), "Simultaneous Observation of Clear Air Convection by a Pulse Radar, an FM-CW Radar, an Acoustic Sounder and an Instrumented Aircraft," Preprints 16th Radar Meteorology Conference, 22-23 April, Houston, Texas, American Meteorological Society, 290-295.

Arnold, A. and Rowland, J.R. (1976), "Fine Scale Observation of Free Convection in the Atmospheric Boundary Layer," Proc. Third Symposium on Atmospheric Turbulence Diffusion and Air Quality, 19-22 October, Raleigh, North Carolina, American Meteorological Society, 1-8.

Ball, F.K. (1960), "Control of Inversion Height by Surface Heating," Quarterly J. Royal Meteorological Society, 86, 483-494.

Briggs, G.A. (1969), Plume Rise, Atomic Energy Commission Review Series, NTIS TID-25075, 81 pp.

Briggs, G.A. (1975), "Plume Rise Predictions," in Lectures on Air Pollution and Environmental Impact Analysis, ed. D.A. Haugen, American Meteorological Society ,Boston, Massachusetts, 59-111.

Busch, N.E. (1977), "Fluxes in the Surface Boundary Layer over the Sea," Proceedings of a NATO Advanced Study Institute, Urbino, Italy, (1975), Pergamon Press, 72-91.

Businger, J.A. (1975), "Interactions of Sea and Atmosphere," Reviews of Geophysics and Space Physics, 13, 720-726, 817-822.

Businger, J.A., Wyngaard, J.C., Izumi, Y. and Bradley, E.F. (1971), "Flux-Profile Relationship in the Atmospheric Surface Layer," J. Atmospheric Sciences, 28, 181-189.

Caughey, S.J., Crease, B.A., Asmakopoulos, D.N. and Cole, R.S. (1977), "Quantitative Bistatic Acoustic Sounding of the Atmospheric Boundary Layer," Quarterly J. Royal Meteorological Society, 104, 147-161.

Crane, G., Panofsky, H.A. and Zeman, O. (1977), "A Model for Dispersion from Area Sources in Convective Turbulence," Atmospheric Environment, 11, 893-900.

Deardorff, J.W. (1970), "A Three Dimensional Numerical Investigation of the Idealized Planetary Boundary Layer," Geophysical Fluid Dynamics, 1, 377-410.

Deardorff, J.W. (1972), "Numerical Investigation of Neutral and Unstable Planetary Boundary Layers," J. Atmospheric Sciences, 29, 91-115.

Deardorff, J.W. (1978), "Prediction of Convective Mixed-Layer Entrainment for Realistic Capping Inversion Structure," J. Atmospheric Sciences, 36, 424-436.

Deardorff, J.W., Willis, G.E. and Stockton, B.H. (1980), "Laboratory Studies of the Entrainment Zone of a Convectively Mixed Layer," J. Fluid Mechanics, 100, 41-64.

Dietz, R.N. and Cote, E.A. (1973), "Tracing Atmospheric Pollutants by Gas Chromatographic Determination of Sulfur Hexafluoride," Environmental Science and Technology, 7, 338-342.

Drivas, P.J. and Shair, F.H. (1974), "A Tracer Study of Pollutant Transport and Dispersion in the Los Angeles Area," Atmospheric Environment, 8, 1155-1163.

Frisch, A.S., Chadwick, R.B., Moninger, W.R. and Young, J.M. (1975), "Observation of Boundary Layer Convection Cells Measured by Dual-Doppler Radar and Echosounder and by Microbarograph Array," Boundary-Layer Meteorology, 3, 199-226.

Hardy, K.R. and Ottersten, H. (1969), "Radar Investigation of Convective Patterns in the Clear Atmosphere," J. Atmospheric Sciences, 26, 666-672.

Heidt, F.D. (1977), "The Growth of the Mixed Layer in a Stratified Fluid Due to Penetrative Convection," Boundary-Layer Meteorology, 12, 439-461.

Houlihan, T.M., Davidson, K.L., Fairall, C.W. and Schacher, G.E. (1978), "Experimental Aspects of a Shipboard System Used in Investigation of Overwater Turbulence and profile Relationships," Naval Post Graduate School Report No. NPS61-78-001 Monterey, California.

Kaimal, J.C., Wyngaard, J.C., Haugen, D.A., Cote´, O.H. and Izumi, Y. (1976), "Turbulence Structure in the Convective Boundary Layer," J. Atmospheric Sciences, 33, 2152-2169.

Kraus, E.B. (1972), Atmosphere-Ocean Interaction, Clarendon Press, Oxford, 275pp.

Konrad, T.G. (1970), "The Dynamics of the Convective Process in Clear Air as Seen by Radar," J. Atmospheric Sciences, 27, 1138-1147.

Lamb, B.K., Lorenzen, A. and Shair, F.H. (1978a), "Atmospheric Dispersion within Coastal Regions - Part I. Tracer Study of Power Plant Emissions from The Oxnard Plain," Atmospheric Environment, 12, 2089-2100.

Lamb, B.K., Shair, F.H. and Smith, T.B. (1978b), "Atmospheric Dispersion within Coastal Regions - Part II. Tracer Study of Industrial Emissions in the California Delta Region," Atmospheric Environment, 12, 2101-2118.

Lamb, R.G., Chen, H.W. and Seinfeld, J.H. (1975), "Numerico-Empirical Analysis of Atmospheric Diffusion Theories," J. Atmospheric Sciences, 32, 1754-1807.

Lyons, W.A. (1975), "Turbulent Diffusion and Pollutant Transport in Shoreline Environments," in Lectures on Air Pollution and Environmental Impact Analysis, ed. D.A. Haugen, American Meteorological Society ,Boston, Massachusetts, 59-111.

Manins, P.C. (1977), "Fumigation and a Laboratory Experiment," Weather, June, 221-228.

McBean, G.A. and MacPherson, J.I. (1975), "Turbulence above Lake Ontario: Velocity and Scalar Statistics," Boundary-Layer Meteorology, 10, 181-197.

McRae, G.J., W.R. Goodin and J.H. Seinfeld (1981), "Development of a Second Generation Mathematical Model for Urban Air Pollution: I Model Formulation," Atmospheric Environment, (In press).

Misra, P.K. (1979), "Dispersion from Tall Stacks into a Shore Line Environment," Atmospheric Environment, 14, 397-400.

Monin, A.S. and Yaglom, A.M. (1971), Statistical Fluid Mechanics: Mechanics of Turbulence, Volume I, MIT Press, Cambridge, Massachusetts, 769 pp.

Orgill, M.M. (1981), "Atmospheric Studies in Complex Terrain: A Planning Guide for Future Studies," Report PNL-3656 prepared by Pacific Northwest Laboratories, Richland, Washington, under U.S. Department of Energy Contract DE-AC06-76RLO 1830.

Raynor, G.S., Michael, P. and SethuRaman, S. (1980), "Meteorological Measurement Methods and Diffusion Models for Use at Coastal Nuclear Reactor Sites," Nuclear Safety, 21, 749-765.

Schacher, G.E., Davidson, K.L., and Fairall, C.W. (1980), "Atmospheric Marine Boundary Layer Mixing rates in the California Coastal Region," Naval Post Graduate School Report No. NPS61-80-003, Monterey, California, 115 pp.

Schacher, G.E., Fairall, C.W., Davidson, K.L., and Houlihan, T.M. (1978), "Experimental Investigation of the Marine Boundary Layer in Support of Air Pollution Studies in the Los Angeles Air Basin," Naval Post Graduate School Report No. NPS61-78-002, Monterey, California, 257 pp.

Schatzmann, M. (1979), "An Integral Model of Plume Rise," Atmospheric Environment, 13, 721-731.

Shair, F.H., Sasaki, E., Carlan, D., Cass, G.R., Goodin, W.R., Edinger, J., and Schacher, G.E. (1981), "Transport and Dispersion of Airborne Pollutants Associated With the Land Breeze-Sea Breeze System," (Submitted for Publication).

Simmonds, P.G., Shoemake, G.R., Lovelock, J.E. and Lord, H.C. (1972), "Improvements in the Determination of Sulfur Hexafluoride for use as a Meteorological Tracer," Analytical Chemistry, 44, 860-863.

Smith, T.B., Marsh, S.L., White, W.H., et al. (1976), "Analysis of the Data from the Three-Dimensional Gradient Study, Final Report submitted to the California Air Resources Board under contracts ARB-4-051 and ARB-4-250, Meteorology Research, Inc., Pasadena, California, and System Applications,

Stull, R.B. (1973), "Inversion Rise Model Based on Penetration Convection," J. Atmospheric Sciences, 30, 1092-1099.

Venkatram A. (1976), "Internal Boundary Layer Development and Fumigation," Atmospheric Environment, 11, 479-482.

Willis, G.E. and Deardorff, J.W. (1976a), "Visual Observations of Horizontal Planforms of Penetration Convection," Proc. Third Symposium on Atmospheric Turbulence Diffusion and Air Quality, 9-12 October, Raleigh, North Carolina, American Meteorological Society, 1-8.

Willis, G.E. and Deardorff, J.W. (1976b), "A Laboratory Model of Diffusion into the Convective Planetary Boundary Layer," Quarterly J. Royal Meteorological Society, 102, 427-445.

Zeman, O. and Tennekes, H. (1977), "Parameterization of the Turbulent Energy Budget at the Top of the Daytime Atmospheric Boundary Layer," J. Atmospheric Sciences, 34.

TABLE 1

BASIC METEOROLOGICAL DATA COLLECTED DURING PERIOD 19-26 JULY 1977*

Date	Time PDT	Humidity(%)	T_a(°C)	T_s(°C)	T_a-T_s(°C)	Q_o(10^3 m/s °K)
19	0000	90	16.4	19.1	-2.75	8.7
19	0020	92	16.0	18.5	-2.53	5.6
19	0100	92	16.0	17.6	-1.61	2.4
19	0140	93	15.9	16.7	-0.80	0.7
19	1620	79	18.7	21.1	-2.39	14.9
19	1650	79	18.5	21.1	-2.57	19.4
19	1710	79	18.3	21.0	-2.72	18.8
19	1730	79	18.1	20.9	-2.77	19.4
19	2000	84	18.2	18.8	-0.59	5.8
19	2040	87	17.5	19.8	-2.26	11.8
19	2120	87	17.5	19.8	-2.26	7.3
19	2140	87	17.6	19.9	-2.33	7.5
19	2200	87	17.6	19.8	-2.20	8.9
20	0700	86	17.0	18.7	-1.67	9.9
20	0740	86	17.3	19.2	-1.93	8.5
20	0900	85	17.8	19.3	-1.46	4.6
20	0920	85	17.9	19.3	-1.42	4.4
20	1240	78	19.0	20.2	-1.20	5.2
20	1300	79	19.0	19.8	-0.78	3.2
20	1320	88	19.0	19.7	-0.63	2.3
20	1800	84	18.8	18.2	0.56	-3.9
20	1900	83	18.3	17.8	0.48	-4.3
20	1920	84	18.4	17.7	0.65	-6.4
20	1940	84	18.3	18.4	-0.12	2.5
20	2000	85	18.2	18.3	-0.09	2.1
20	2020	86	17.7	18.3	-0.56	3.7
20	2040	87	17.9	18.3	-0.45	2.5
20	2120	88	17.8	18.2	-0.41	2.3
20	2140	89	17.7	18.2	-0.53	2.8
20	2220	90	17.6	19.0	-1.38	4.8
20	2230	91	17.6	18.4	-0.83	2.7
20	2300	91	17.2	18.2	-1.00	2.9

*Source: Schacher et al. (1980)

TABLE 1 (Continued)

BASIC METEOROLOGICAL DATA COLLECTED DURING PERIOD 19-26 JULY 1977

Date	Time PDT	Humidity(%)	T_a(°C)	T_s(°C)	T_a-T_s(°C)	Q_o(10^3 m/s °K)
21	0000	94	16.6	17.2	-0.63	2.5
21	0040	94	16.2	16.9	-0.70	2.5
21	0100	93	15.9	16.6	-0.72	2.0
21	0405	98	16.2	17.7	-1.46	6.3
21	0425	97	16.4	18.1	-1.65	6.2
21	0445	96	16.8	18.4	-1.57	6.0
21	0505	94	17.1	18.4	-1.33	4.5
21	0545	91	17.4	18.2	-0.81	2.2
21	0605	89	17.4	18.3	-0.84	0.7
21	0645	89	17.3	18.3	-0.96	2.0
21	0705	89	17.3	18.2	-0.86	2.4
21	0845	91	17.7	19.0	-1.31	6.4
21	0905	89	17.8	18.9	-1.14	3.9
21	0945	89	17.5	18.8	-1.26	2.8
21	1005	88	17.4	18.2	-0.72	2.1
21	1025	88	17.6	18.5	-0.38	0.8
21	1045	88	17.6	18.4	-0.80	1.6
21	1105	89	17.4	17.7	-0.33	2.1
21	1305	90	17.7	17.7	-0.05	2.2
21	1325	90	17.5	17.7	-0.24	3.0
21	1345	90	17.5	17.9	-0.40	3.0
21	1405	90	17.7	18.2	-0.54	4.6
21	1505	88	18.2	18.9	-0.68	7.9
21	1620	86	18.3	18.8	-0.47	6.6
21	1720	85	18.0	18.7	-0.69	6.4
21	1945	79	18.6	19.9	-1.30	10.4
21	2030	85	18.2	19.8	-1.66	7.5
21	2110	84	18.3	19.7	-1.35	3.4
21	2130	85	18.3	19.5	-1.21	3.8

TABLE 1 (Continued)

BASIC METEOROLOGICAL DATA COLLECTED DURING PERIOD 19-26 JULY 1977

Date	Time PDT	Humidity(%)	T_a(°C)	T_s(°C)	T_a-T_s(°C)	Q_o(10^3 m/s °K)
22	0550	93	17.1	17.3	-0.19	0.5
22	0610	94	16.9	17.2	-0.34	0.7
22	0710	96	16.5	17.3	-0.77	0.5
22	0730	97	16.6	17.3	-0.68	0.4
22	0750	97	16.5	17.3	-0.76	0.5
22	0810	97	16.7	17.3	-0.57	0.3
22	0830	96	16.6	17.3	-0.72	2.1
22	0910	97	16.5	17.3	-0.78	1.4
22	0930	97	16.6	17.3	-0.71	0.8
22	1030	96	17.1	18.5	-1.46	4.6
22	1050	94	17.5	18.6	-1.09	1.4
23	1440	87	19.2	18.2	0.92	-1.4
23	1505	85	19.5	18.7	0.76	-2.9
23	1645	83	19.9	20.4	-0.43	5.1
23	1725	85	19.1	19.2	-0.08	1.9
23	1745	87	18.8	19.1	-0.28	1.2
23	2340	90	18.5	18.0	0.53	-0.5
24	0040	91	19.1	18.6	0.50	-0.7
24	0100	90	19.0	18.6	0.39	-0.5
24	0120	90	19.0	18.7	0.28	-0.3
24	0240	87	19.0	18.7	0.25	-0.3
24	0300	86	19.0	18.7	0.28	-0.3
24	0420	88	18.8	18.7	0.06	0.0
24	1000	78	19.3	19.2	0.06	0.5
25	2220	83	19.3	17.7	1.57	-8.8
25	2320	84	19.1	17.9	1.27	-7.1
26	0420	90	18.6	18.1	0.49	-0.2

TABLE 2

ADDITIONAL DATA AND CALCULATED RESULTS FOR PERIOD 19-26 JULY 1977*

Date	Time PDT	u (m/s)	θ (deg)	Z_i/L	u_* (m/s)	T_* (^oK)	Z_i (m)	w_* (m/s)	λ (min)
19	0000	1.5	283	-4.840	0.060	-0.117	280	0.436	11
19	0020	1.0	308	-8.206	0.044	-0.104	330	0.397	14
19	0100	0.5	317	-18.190	0.025	-0.075	320	0.296	18
19	0140	0.3	11	-29.206	0.014	-0.035	190	0.166	19
19	1620	3.1	294	-1.125	0.112	-0.077	470	0.585	13
19	1650	3.9	272	-0.754	0.142	-0.085	500	0.663	13
19	1710	3.6	275	-0.929	0.132	-0.093	490	0.659	12
19	1730	3.7	285	-0.889	0.136	-0.096	480	0.665	12
19	2000	4.4	277	-0.216	0.156	-0.023	500	0.477	17
19	2040	3.0	280	-1.134	0.108	-0.082	540	0.597	15
19	2120	1.5	5	-4.174	0.060	-0.092	590	0.525	19
19	2140	1.5	318	-4.291	0.060	-0.096	600	0.534	19
20	0700	3.6	285	-0.542	0.129	-0.051	160	0.369	7
20	0740	2.5	260	-1.433	0.089	-0.068	230	0.400	10
20	0900	1.5	250	-2.852	0.058	-0.053	160	0.290	9
20	0920	1.5	250	-2.502	0.058	-0.044	180	0.286	10
20	1240	2.0	195	-1.645	0.071	-0.036	360	0.385	16
20	1300	1.8	206	-1.459	0.064	-0.020	360	0.332	18
20	1320	2.0	220	-0.773	0.069	-0.013	280	0.264	18
20	1800	7.2	186	0.045	0.259	0.036	80		
20	1900	6.2	275	0.079	0.213	0.042	140		
20	1920	7.2	250	0.058	0.257	0.041	160		
20	1940	7.2	270	-0.004	0.267	0.013	260	0.069	
20	2000	5.7	270	-0.024	0.203	0.007	280	0.228	20
20	2020	5.1	270	-0.056	0.183	-0.001	240	0.273	15
20	2040	3.6	280	-0.158	0.123	-0.005	200	0.248	13
20	2120	3.6	270	-0.150	0.123	-0.005	240	0.258	15
20	2140	3.5	260	-0.186	0.120	-0.009	240	0.272	15
20	2220	2.0	280	-1.606	0.071	-0.048	340	0.378	15
20	2230	2.0	290	-0.931	0.069	-0.023	340	0.305	19
20	2300	2.3	302	-0.356	0.080	-0.030	300	0.328	15

*Source: Schacher et al. (1980)

TABLE 2 (Continued)

ADDITIONAL DATA AND CALCULATED RESULTS FOR PERIOD 19-26 JULY 1977

Date	Time PDT	u (m/s)	θ (deg)	Z_i/L	u_* (m/s)	T_* (^oK)	Z_i (m)	w_* (m/s)	λ (min)
21	0000	2.6	255	-0.470	0.087	-0.020	280	0.288	16
21	0040	2.6	259	-0.441	0.087	-0.019	310	0.290	18
21	0100	1.8	305	-0.876	0.063	-0.019	200	0.227	15
21	0120	1.0	141	-1.656	0.039	-0.014	270	0.193	23
21	0405	3.1	85	-0.595	0.108	-0.048	240	0.370	11
21	0425	2.5	125	-1.106	0.088	-0.058	320	0.406	13
21	0445	2.6	142	-0.994	0.090	-0.054	380	0.425	15
21	0505	2.1	125	-1.443	0.073	-0.049	360	0.380	16
21	0545	1.5	160	-1.497	0.056	-0.025	455	0.319	24
21	0605	0.2	160	-43.572	0.012	-0.031	460	0.213	36
21	0645	1.0	100	-3.625	0.040	-0.030	480	0.310	26
21	0705	1.5	100	-1.691	0.055	-0.026	460	0.326	23
21	0845	3.1	95	-0.583	0.108	-0.040	475	0.457	17
21	0905	2.1	91	-1.158	0.072	-0.032	430	0.368	19
21	0945	1.0	129	-4.270	0.041	-0.040	360	0.310	19
21	1005	1.5	135	-1.164	0.055	-0.014	310	0.252	21
21	1025	0.2	200	-39.449	0.012	-0.024	300	0.176	28
21	1045	0.8	235	-3.474	0.033	-0.015	280	0.212	22
21	1105	3.6	270	-0.035	0.120	0.006	260	0.143	30
21	1305	7.2	258	0.006	0.264	0.012	180		
21	1325	7.0	260	0.000	0.256	0.009	210		
21	1345	6.5	280	-0.003	0.237	0.008	200	0.079	42
21	1405	6.7	285	-0.020	0.246	0.000	200	0.244	14
21	1505	6.5	280	-0.045	0.240	-0.007	200	0.318	10
21	1620	7.0	260	-0.021	0.260	0.003	200	0.258	13
21	1720	5.5	270	-0.058	0.198	-0.003	120	0.239	8
21	1945	4.0	250	-0.397	0.144	-0.038	250	0.428	10
21	2030	2.5	225	-1.328	0.089	-0.059	150	0.336	7
21	2110	1.0	220	-5.585	0.042	-0.053	300	0.325	15
21	2130	1.5	220	-2.618	0.056	-0.043	310	0.341	15

TABLE 2 (Continued)

ADDITIONAL DATA AND CALCULATED RESULTS FOR PERIOD 19-26 JULY 1977

Date	Time PDT	u (m/s)	θ (deg)	Z_i/L	u_* (m/s)	T_* (^oK)	Z_i (m)	w_* (m/s)	λ (min)
22	0550	2.0	130	-0.209	0.065	0.000	205	0.143	24
22	0610	1.5	130	-0.550	0.053	-0.006	220	0.169	22
22	0710	0.2	140	-35.247	0.012	-0.030	240	0.157	26
22	0730	0.2	120	-29.493	0.012	-0.024	240	0.144	28
22	0750	0.2	140	-32.846	0.012	-0.028	240	0.152	26
22	0810	0.2	150	-21.592	0.011	-0.015	245	0.126	33
22	0830	2.1	180	-0.631	0.070	-0.018	230	0.238	16
22	0910	1.0	307	-2.365	0.040	-0.024	210	0.205	17
22	0930	0.5	270	-6.285	0.023	-0.020	220	0.165	22
22	1010	2.6	260	-0.763	0.089	-0.040	240	0.330	12
22	1030	2.0	250	-1.369	0.071	-0.045	260	0.326	13
22	1050	0.5	305	-10.055	0.024	-0.033	260	0.213	20
23	1440	2.5	250	1.332	0.050	0.031	280		
23	1505	3.9	215	0.285	0.114	0.039	310		
23	1645	4.6	275	-0.086	0.163	0.001	320	0.307	17
23	1725	4.9	262	-0.011	0.170	0.012	355	0.112	
23	1745	2.1	244	-0.268	0.068	0.004	350	0.188	31
23	2340	1.7	260	1.943	0.029	0.017	500		
24	0040	2.1	281	0.527	0.052	0.017	155		
24	0100	1.8	270	0.776	0.043	0.017	120		
24	0120	1.5	236	0.767	0.037	0.014	170		
24	0240	1.7	140	0.381	0.046	0.016	120		
24	0300	1.5	136	0.455	0.041	0.016	160		
24	0420	1.0	210	0.044	0.032	0.011	140		
24	1000	1.0	269	-0.091	0.034	0.021	165		
25	2220	5.0	270	0.340	0.150	0.068	160		
25	2320	5.0	280	0.231	0.157	0.054	160		
26	0420	1.4	340	3.147	0.019	0.012	90		

TABLE 3

CONVECTIVE MIXING TIMES BASED ON TURBULENCE INTENSITIES FOR 22 JULY 1977

Date	Time PDT	Z_i/L	u_* (m/s)	Z_i (m)	R_i	ϵ (10^{-4} m/s^3)	$\left[\frac{Z_i^2}{\epsilon}\right]^{\frac{1}{3}}$ (min)	$\left[\frac{Z_i^2}{\epsilon R_i}\right]^{\frac{1}{3}}$ (min)
22	0550	-0.209	0.065	205	-0.04	1.8	10	30
22	0610	-0.550	0.053	220	-0.09	3.6	8	19
22	0710	-35.247	0.012	240	-0.16	3.6	9	17
22	0730	-29.493	0.012	240	-0.08	4.0	9	20
22	0750	-32.846	0.012	240	-0.18	2.9	10	17
22	0810	-21.592	0.011	245	-0.21	5.1	8	14
22	0830	-0.631	0.070	230	-0.10	4.6	8	17
22	0910	-2.365	0.040	210	-0.02	7.1	7	24
22	0930	-6.285	0.023	220	-0.03	7.3	7	22

FIGURE CAPTIONS

Figure 1. Sulfur hexafluoride (SF_6) measurements made on board R/V Arcania 22 July 1977 coordinated with ship course and possible plume trajectories derived from surface and elevated wind measurements. (● Release site, • On shore monitoring sites)

Figure 2 Sulfur hexafluoride (SF_6) measurements made on board R/V Arcania 24 July 1977 coordinated with ship course and possible plume trajectories derived from surface and elevated wind measurements. (● Release site, • On shore monitoring sites)

Figure 3. Intermittent Entrainment of Tracer Material by Convective Cells

Figure 4. Schematic Representation of (a) Fumigation Process and (b) Notation for Mixing Model

Figure 5. Distribution of Convective Mixing Times (a) Daytime Conditions Over land (Source: Smith et al. 1976) (b) Nighttime Conditions Over ocean

Figure 6. Vertical Turbulent Diffusivity Profile for Unstable Conditions (Source: McRae et al. 1981)

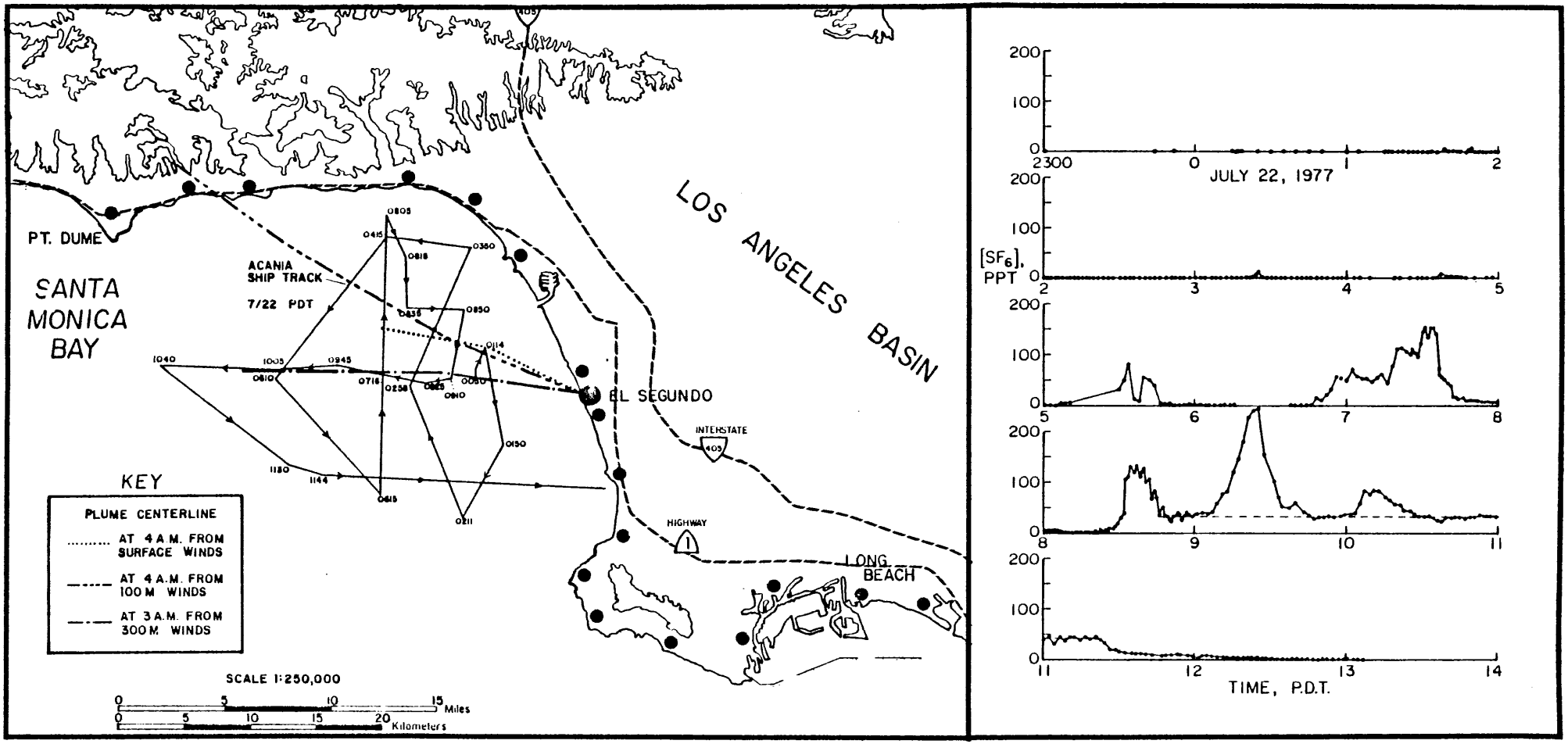
PT. DUME
SANTA MONICA BAY
ACANIA SHIP TRACK
7/22 PDT
LOS ANGELES BASIN
EL SEGUNDO
INTERSTATE 405
HIGHWAY 1
LONG BEACH
KEY
PLUME CENTERLINE
AT 4 A.M. FROM SURFACE WINDS
AT 4 A.M. FROM 100 M WINDS
AT 3 A.M. FROM 300 M. WINDS
SCALE 1:250,000
0 5 10 15 Miles
0 5 10 15 20 Kilometers
JULY 22, 1977
[SF6], PPT
TIME, P.D.T.

Figure 1

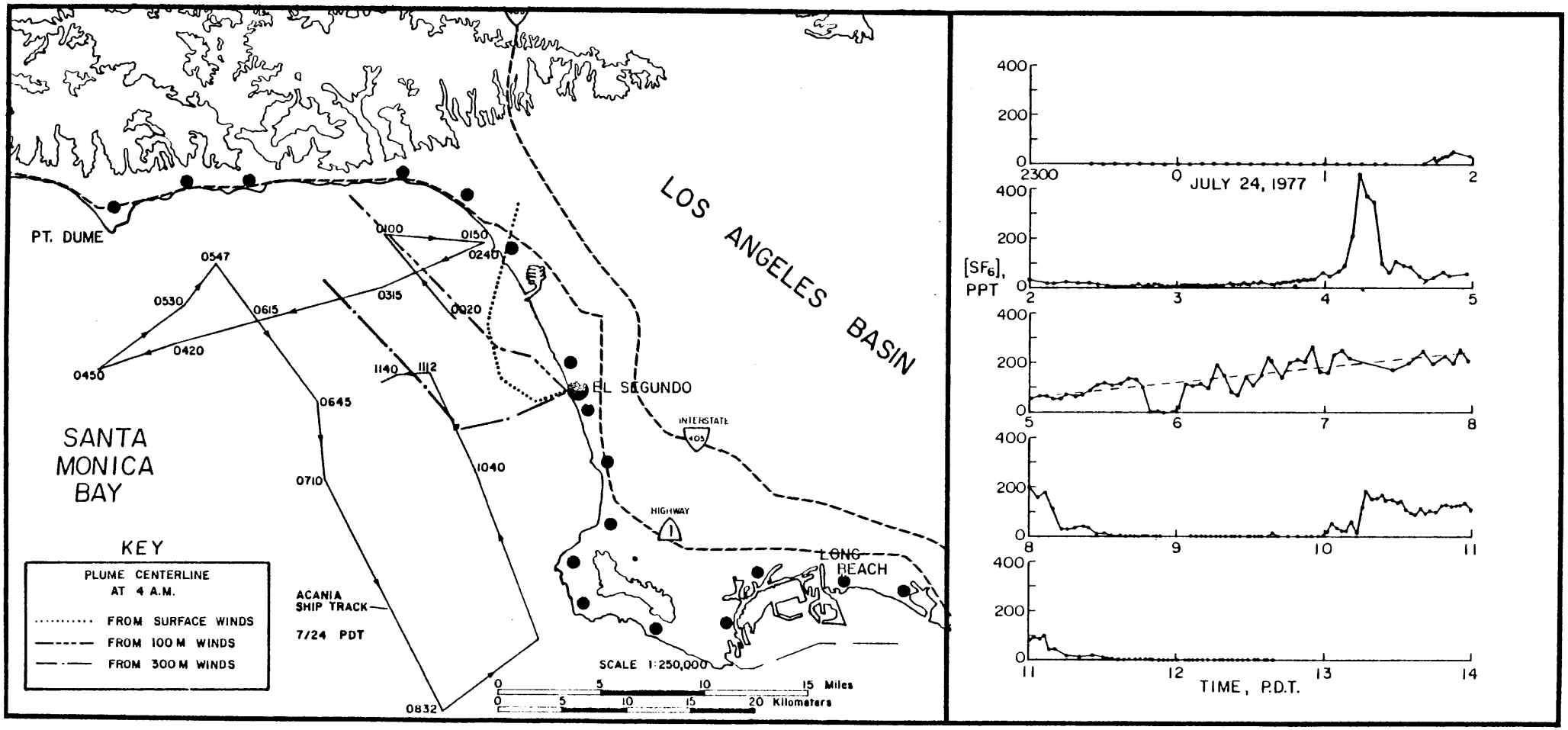
PT. DUME
0547
0530
0615
0420
0450
0315
0100
0150
0240
0020
1140
1112
0645
0710
1040
0832
SANTA MONICA BAY
LOS ANGELES BASIN
EL SEGUNDO
INTERSTATE 405
HIGHWAY 1
LONG BEACH
KEY
PLUME CENTERLINE AT 4 A.M.
FROM SURFACE WINDS
FROM 100 M WINDS
FROM 300 M WINDS
ACANIA SHIP TRACK
7/24 PDT
SCALE 1:250,000
0 5 10 15 Miles
0 5 10 15 20 Kilometers
400
200
0
2300
0
JULY 24, 1977
1
2
[SF6], PPT
3
4
5
6
7
8
9
10
11
12
13
14
TIME, P.D.T.

Figure 2

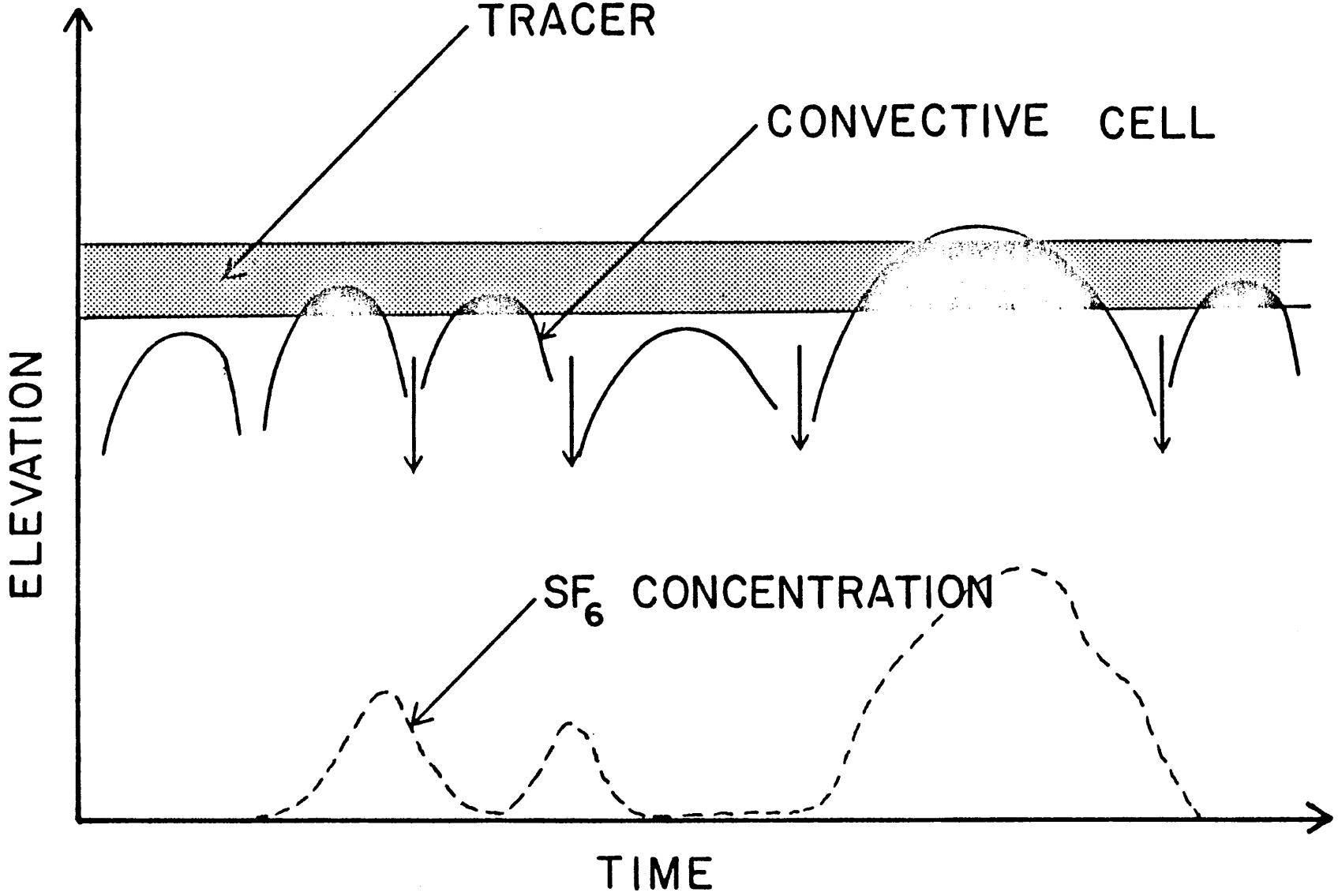

Figure 3

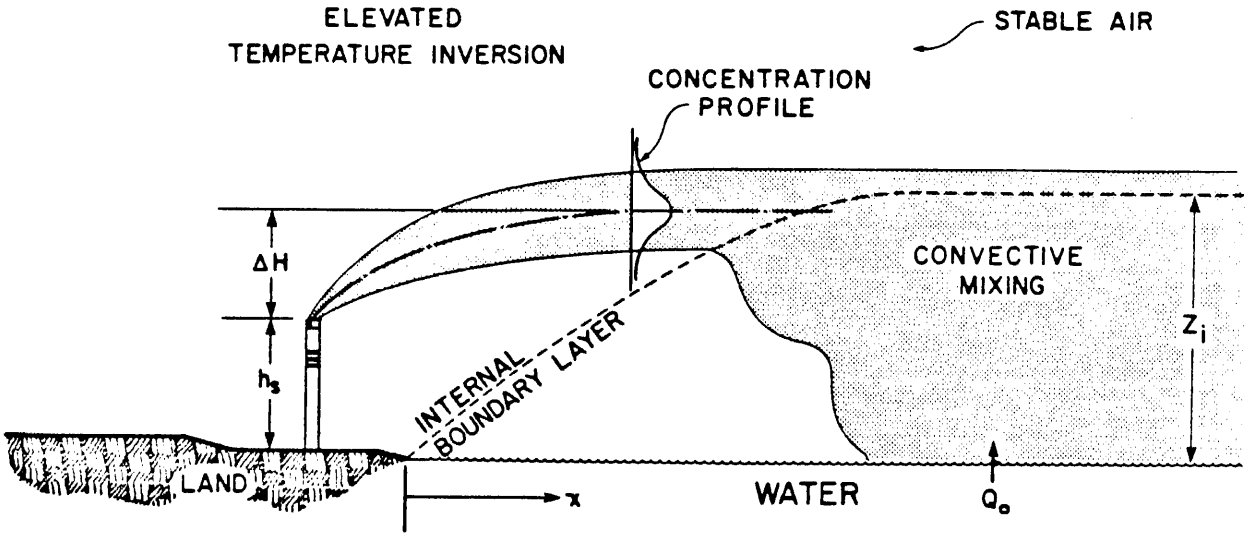
ELEVATED
TEMPERATURE INVERSION
STABLE AIR
CONCENTRATION
PROFILE
ΔH
h_s
CONVECTIVE
MIXING
Z_i
INTERNAL
BOUNDARY LAYER
LAND
x
WATER
Q_o

(a)

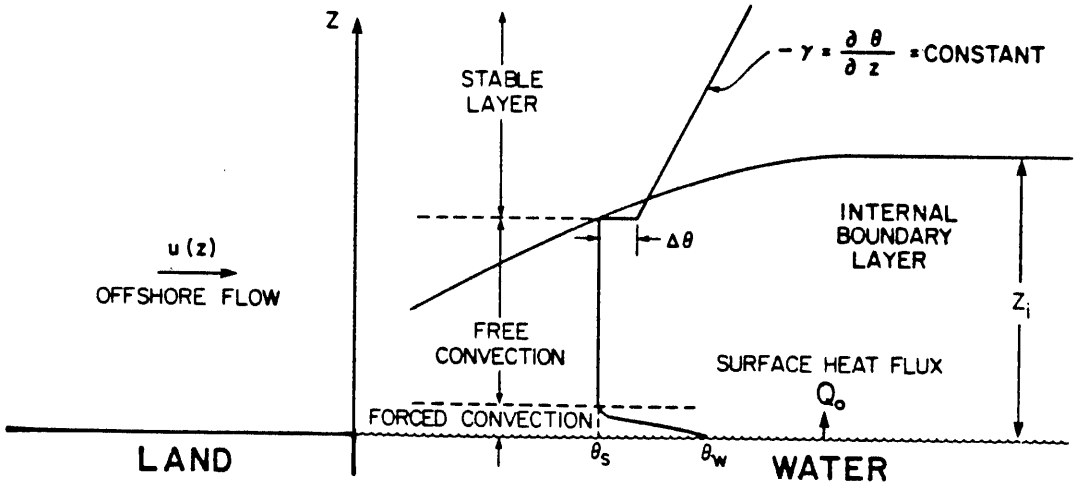
z
STABLE
LAYER
$-\gamma = \frac{\partial \theta}{\partial z}$ =CONSTANT
u(z)
OFFSHORE FLOW
$\Delta\theta$
INTERNAL
BOUNDARY
LAYER
Z_i
FREE
CONVECTION
SURFACE HEAT FLUX
Q_o
FORCED CONVECTION
LAND
θ_s
θ_w
WATER

(b)

Figure 4

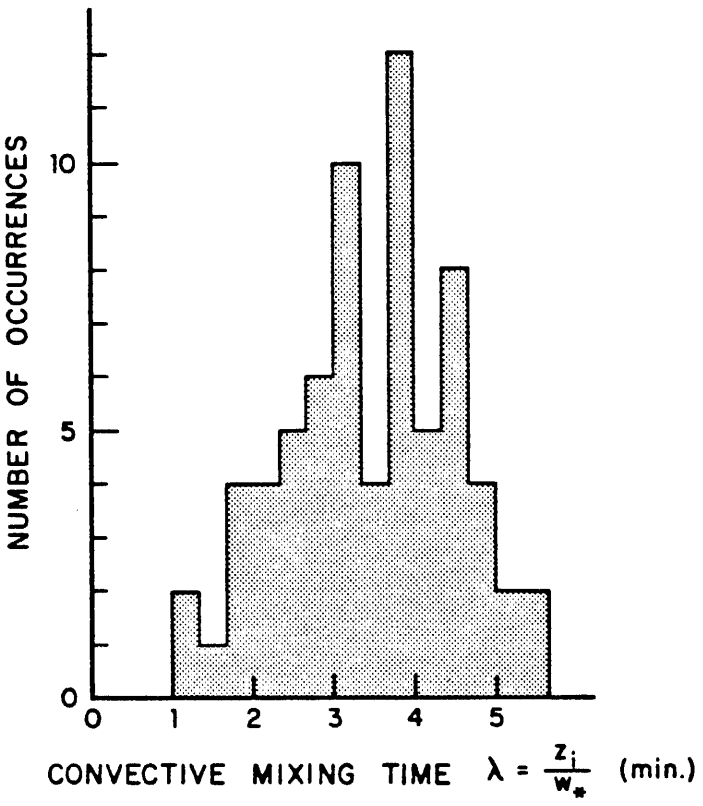
NUMBER OF OCCURRENCES
0
5
10
0 1 2 3 4 5
CONVECTIVE MIXING TIME $\lambda = \frac{z_i}{w_*}$ (min.)

(a)

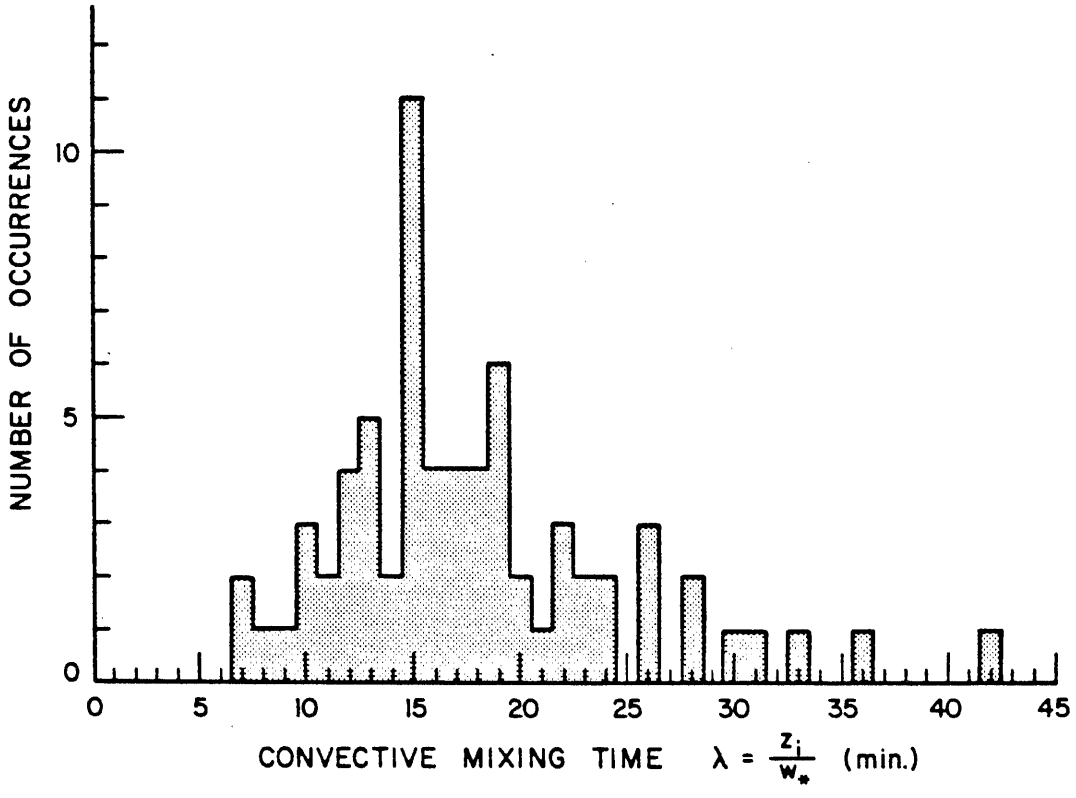
NUMBER OF OCCURRENCES
0
5
10
0 5 10 15 20 25 30 35 40 45
CONVECTIVE MIXING TIME $\lambda = \frac{z_i}{w_*}$ (min.)

(b)

Figure 5

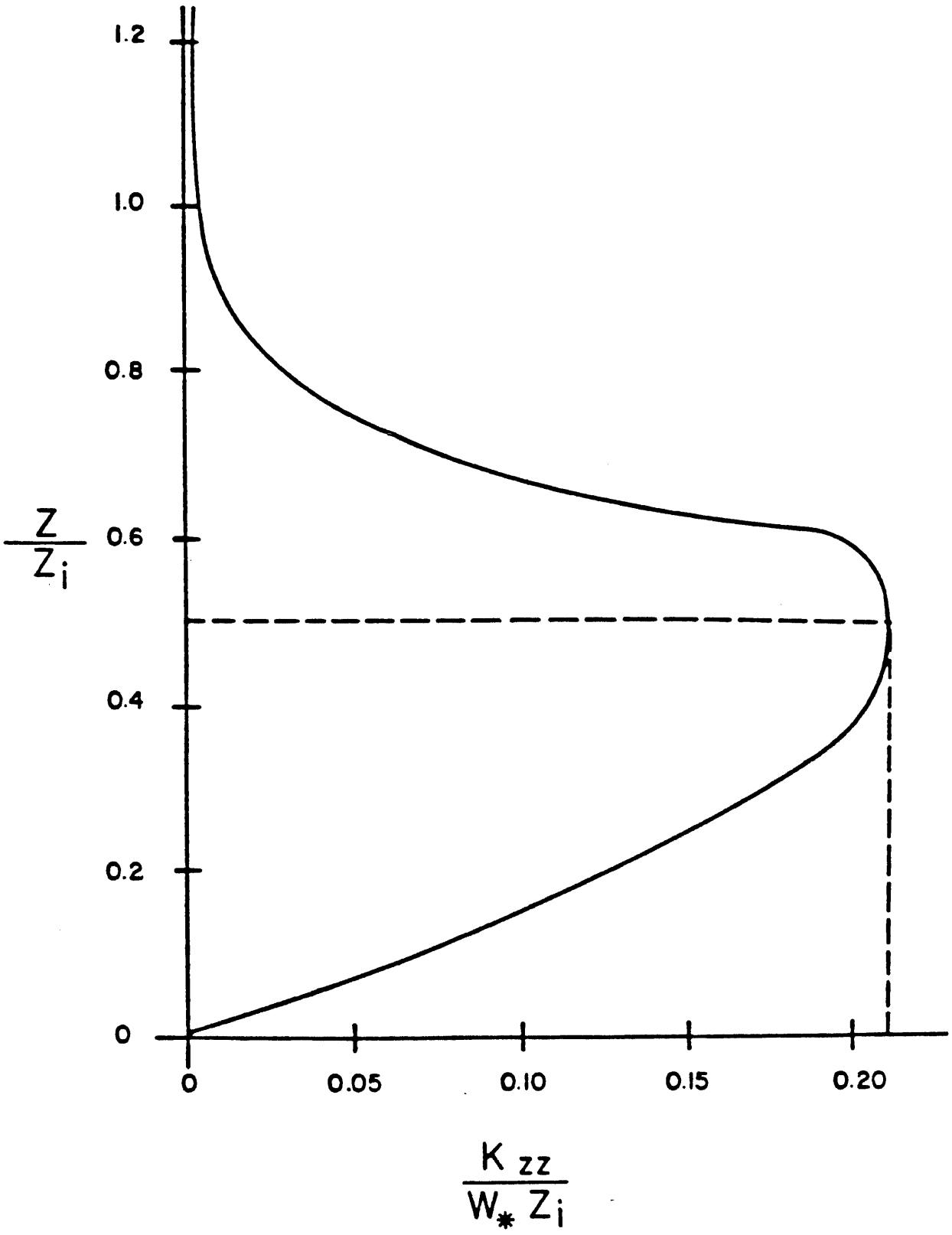

Figure 6